NASA TECHNICAL REPORT

NASA TR R-250

NASA TR R-250

HYPERSONIC AERODYNAMIC PERFORMANCE OF MINIMUM-WAVE-DRAG BODIES

by Bernard Spencer, Jr., and Charles H. Fox, Jr.

Langley Research Center
Langley Station, Hampton, Va.

NATIONAL AERONAUTICS AND SPACE ADMINISTRATION • WASHINGTON, D. C. • NOVEMBER 1966

ERRATA

NASA Technical Report R-250

HYPERSONIC AERODYNAMIC PERFORMANCE OF MINIMUM-WAVE-DRAG BODIES

By Bernard Spencer, Jr., and Charles H. Fox, Jr.

November 1966

Page 6, line 1: The word "Positive" near the end of this line should be "Negative."

Page 24 and 25: In figures 3(a) and 3(b), the signs should be reversed on all $C_{A,b}$ scales; that is, positive values of $C_{A,b}$ should be negative and negative values of $C_{A,b}$ should be positive.

Page 43: In the key identifying symbols (fig. 7(d)), the value of ".001672" for the V/l^3 corresponding to $F = 7.98$ should be ".006172."

NASA-Langley, 1967

Issued 6-30-67

NASA TR R-250

HYPERSONIC AERODYNAMIC PERFORMANCE OF MINIMUM-WAVE-DRAG BODIES

By Bernard Spencer, Jr., and Charles H. Fox, Jr.

Langley Research Center
Langley Station, Hampton, Va.

NATIONAL AERONAUTICS AND SPACE ADMINISTRATION

For sale by the Clearinghouse for Federal Scientific and Technical Information
Springfield, Virginia 22151 – Price $2.00

HYPERSONIC AERODYNAMIC PERFORMANCE OF MINIMUM-WAVE-DRAG BODIES

By Bernard Spencer, Jr., and Charles H. Fox, Jr.
Langley Research Center

SUMMARY

An experimental investigation has been made at a Mach number of 10.03 to determine the longitudinal aerodynamic characteristics of a series of power-law bodies having values of the exponent of 0.25, 0.50, 0.66, 0.75, and 1.00, and a theoretical hypersonic minimum-wave-drag body. The bodies had the same length and volume, and the theoretical body shape was determined under the geometric constraints of prescribed length and volume. For each body, cross-sectional shape was altered from circular to elliptic, while maintaining a constant longitudinal distribution of cross-sectional area. Results of the investigation may be summarized in the following observations.

For the series of power-law bodies tested, a minimum in the variation of zero-lift drag with body exponent occurs for an exponent of 0.66 for ellipse ratios of 1.0 or 2.0; a resultant maximum in the variation of maximum lift-drag ratio with body exponent was also found for an exponent of 0.66 for ellipse ratios of either 1.0 or 2.0. The zero-lift drag characteristics of the theoretical minimum-wave-drag body are slightly lower than those noted for the 0.66-power body, and the resultant maximum lift-drag-ratio characteristics are somewhat higher for ellipse ratios of either 1.0 or 2.0.

The effects of increasing ellipticity, for a given power body or the theoretical body, resulted in an almost constant incremental increase in maximum lift-drag ratio, independent of body longitudinal contour; these increases were primarily a result of the improved lift characteristics.

AUTHOR

INTRODUCTION

Generalized theoretical and experimental research directed toward eventual development of aerodynamically efficient vehicles capable of operation at hypersonic speeds is presently being performed by the National Aeronautics and Space Administration (NASA) and others. Results of these studies are directly applicable to the possible development of hypersonic cruise or glide configurations requiring considerable range capability (ref. 1) and, to a certain extent, manned spacecraft expected to possess immediate recall capability with extensive recovery footprints, as noted in reference 2. The question

arises, however, as to whether the vehicle should be winglike or bodylike; and when considered from aerodynamic performance considerations only, the former is considerably more attractive. (See ref. 3.) The consideration of volumetric efficiency and resultant structural weight, however, would tend to dictate that the vehicle be bodylike in structure. In an effort to combine the favorable volume-weight efficiency of body shapes with a high degree of aerodynamic performance, numerous studies have been made on lifting-body configurations from low subsonic through hypersonic speeds. (See refs. 4 to 15.)

The present studies were initiated as a continuation of these early studies in order to provide information relating to methods of improving the aerodynamic performance of a certain class of lifting-body configurations at hypersonic speeds. Two approaches have been followed in the present study: (1) to minimize the zero-lift pressure drag of basic circular-cross-section bodies of prescribed length and volume, and (2) to increase the planform area of these bodies by altering the basic circular cross section to an ellipse while maintaining constant length and volume. The basic or primary bodies tested were the theoretical zero-lift hypersonic minimum-wave-drag bodies as determined under the geometric constraints of given length and volume by the method described in reference 16 for circular cross section and in reference 17 for elliptic cross section. The longitudinal aerodynamic characteristics of these minimum-wave-drag bodies are compared with those for a series of circular and elliptic power-law bodies (i.e., the lateral ordinate is defined by a function of the longitudinal ordinate raised to an exponent) having the same length and volume as the theoretical bodies. Power-law bodies are useful in that for certain combinations of prescribed geometric constraints, a power relationship offers an approximation to the body shape of minimum wave drag (for example, the exponent 0.75 for given length and base diameter, refs. 16 to 18; 0.66 for given length and volume, ref. 19; and 1.0 for given base diameter and wetted area, ref. 16 or 18). The Mach number of the present investigation was 10.03, corresponding to a Reynolds number (based on body length) of 1.40×10^6. The angle-of-attack range was from approximately -8° to 40° at 0° of sideslip. The data of the present investigation are also presented in summary form along with transonic results (ref. 11) and supersonic results (ref. 14) as a function of Mach number.

Also included as an appendix is a systematic study of the solutions of the parametric equations used to determine the minimum-wave-drag shape; it includes the effects of both fineness ratio and ellipticity for the imposed geometric constraints of fixed length and volume. Simple design charts are presented which enable the rapid and accurate determination of the minimum-wave-drag body ordinates.

SYMBOLS

Longitudinal data are presented about the stability axes, and all coefficients are nondimensionalized with respect to the projected planform area and length of each body, unless otherwise noted. The longitudinal location of the moment reference point was selected as 66.67 percent of body length for each configuration; the vertical moment reference point was located on the body center line.

A — aspect ratio, $\left(\frac{2a_{max}}{S}\right)^2$

A_b — body base area, sq ft (meters^2)

A_x — local cross-sectional area of body, sq ft (meters^2)

a — semimajor (horizontal) axis of elliptic-cross-section bodies (radius for $a/b = 1.0$ bodies), $a = \left(\frac{a_{max}}{l^n}\right)x^n$, feet (meters)

a_{max} — body maximum semispan, feet (meters)

b — semiminor (vertical) axis of elliptic-cross-section bodies, feet (meters)

$C_{A,b}$ — base axial-force coefficient, $\frac{p_b - p_\infty}{q}\frac{A_b}{S}$

C_D — drag coefficient, $\frac{Drag}{qS}$

$C_{D,min}$ — minimum drag coefficient

$C'_{D,min}$ — minimum drag coefficient with base axial force corrected to free-stream conditions

C_L — lift coefficient, $\frac{Lift}{qS}$

C_{L_α} — lift-curve slope at $\alpha \approx 0^o$, per degree

C_m — pitching-moment coefficient, $\frac{Pitching\ moment}{qSl}$

C_{m_α} — longitudinal-stability parameter at $\alpha \approx 0^o$, per degree

C_N — normal-force coefficient, $\frac{Normal\ force}{qS}$

C_{N_α}	normal-force-curve slope at $\alpha \approx 0^o$, per degree
C_p	pressure coefficient, $\frac{p - p_\infty}{q}$
$\frac{D}{q\ell^2}$	minimum drag coefficient based on body length
L/D	lift-drag ratio
$(L/D)_{max}$	maximum lift-drag ratio
$(L/D)'_{max}$	maximum lift-drag ratio with base axial force corrected to free-stream conditions
$\left(\frac{L}{q\ell^2}\right)_\alpha$	lift-curve slope at $\alpha \approx 0^o$ based on body length, per degree
ℓ	total body length, 0.8333 foot (0.254 meter)
M	free-stream Mach number
n	power-body exponent
p	static pressure, lb/sq ft (newtons/meter^2)
p_b	static pressure at model base, lb/sq ft (newtons/meter^2)
p_∞	free-stream static pressure, lb/sq ft (newtons/meter^2)
q	free-stream dynamic pressure, lb/sq ft (newtons/meter^2)
S	body projected-planform area, sq ft (meters^2)
S_{wet}	total wetted area of body (excluding base area), sq ft (meters^2)
V	volume of body, cu ft (meters^3)
V/ℓ^3	volume-to-length-cubed ratio, constant for all bodies (0.010496)
x	longitudinal coordinate with origin at body nose, feet (meters)
x_{cg}	longitudinal coordinate of moment reference point, feet (meters)

x_{cp}/l longitudinal center-of-pressure location, $\frac{x_{cg}}{l} - \left(\frac{C_{m_\alpha}}{C_{N_\alpha}}\right)_{\alpha \approx 0^o}$

y lateral coordinate of body (parallel to minor axis for elliptical cross-section bodies), feet (meters)

y' local body slope, $\frac{dy}{dx}$

α angle of attack, degrees

MODELS

The models used in the present investigation were of 12 different body shapes. Details of the models are presented in figure 1(a), and the various geometric parameters associated with each body tested are given in figure 1(b). Photographs of the body shapes tested are presented as figure 2.

All the bodies used were symmetrical and had either circular or elliptic cross sections; that is, horizontal-to-vertical axis ratios a/b of 1.0 (fig. 2(a)) and 2.0 (fig. 2(b)), which were held constant along the length of the body. The planform of the power-law bodies was defined by the relation $a = \left(\frac{a_{max}}{l^n}\right)x^n$ with values of the exponent n of 0.25, 0.50, 0.66, 0.75, and 1.00. The planforms of the bodies designated as the theoretical hypersonic minimum-wave-drag shape were defined as described in references 16 and 17 and do not conform to a power relation. For each power body or the theoretical minimum-wave-drag body, a constant longitudinal distribution of cross-sectional area was maintained in altering cross-section shape from circular to elliptic.

APPARATUS, TESTS, AND CORRECTIONS

The present investigation was made in the Langley 15-inch hypersonic flow apparatus at a Mach number of 10.03. A brief description of this facility is given in reference 20. Forces and moments were measured with a sting-supported six-component water-cooled strain-gage balance. The angle-of-attack range was from approximately -8^o to 40^o at 0^o of sideslip.

Tests were made at a stagnation temperature of approximately 1340^o F (2685^o K) and a stagnation pressure of approximately 1000 lb/sq in. (6895 kN/sq m) corresponding to a free-stream Reynolds number, based on body length, of 1.40×10^6.

The angle of attack has been corrected for sting and balance deflections under load. Base axial-force measurements have been obtained for each body tested and are

presented in coefficient form in figure 3 as a function of angle of attack. Positive $C_{A,b}$ values are noted at $\alpha = 0^{o}$, due to sting-induced effects. These values are less than 0.0008, however, and are within estimated balance accuracy; they have, therefore, not been applied to the basic data of figures 4 and 5. Similarly, $C_{A,b}$ values approach 0 near the α value for $(L/D)_{max}$, and when applied to C_L and C_D with sine and cosine functions of α, have only minor effects on the $(L/D)_{max}$ values obtained. However, the $C'_{D,min}$ and $(L/D)'_{max}$ values at $M = 10.03$, presented in figures 6(d) and (f), respectively, have been corrected to free-stream static conditions on the model base for correlation with supersonic results that have been corrected for base axial-force effects.

Since the data of the present investigation have been correlated with data obtained in other facilities, the following table is furnished to give pertinent test conditions along with facility designation:

TABLE I.- TEST CONDITIONS

Facility	M	Reynolds number (based on body length)	Reference
Langley high-speed 7- by 10-foot tunnel	0.50	6.25×10^6	11
	.80	8.33	
	.90	8.54	
	.95	8.73	
	1.00	8.86	
	1.12	9.00	
Langley Unitary Plan wind tunnel	1.50 to 4.63	5.73	14
Langley 15-inch hypersonic flow apparatus	10.03	1.40	Present paper

PRESENTATION OF RESULTS

The following table is presented as an aid in locating a particular set of experimental results.

DISCUSSION

Previous Results Relating to Minimum-Drag Bodies

The problem of determining the shape of a circular axisymmetric body of minimum pressure drag in a hypersonic inviscid flow was considered by Eggers, et al. (ref. 16), for various combinations of imposed geometric constraints. Using Newton's law of resistance, stated mathematically as $C_p = \frac{2(y')^2}{1 + (y')^2}$, the variational calculus was employed to obtain solutions from which a body shape could be found which minimized the pressure drag, while satisfying the prescribed input geometric conditions. For the particular case of given length and base diameter, Eggers found graphically that a power relationship in $y \propto x^n$ closely approximated the solution of the minimum-drag body, especially at the higher fineness ratios, the exponent value being $n = 0.75$ (ref. 16). Miele (ref. 18) by assuming a slender-body approximation (that is, $(y')^2 << 1.0$) modified the Newtonian pressure coefficient to $C_p = 2(y')^2$, and was therefore able to obtain analytic solutions to the minimum-wave-drag shapes. He found $n = 0.75$ to be an exact slender-body solution satisfying the Euler-Lagrange equations for the input geometric constraints of given length and base diameter. An experimental investigation was made at $M = 6.00$ (ref. 16) on a series of power-law bodies, including $n = 0.25$, 0.50, 0.75, and 1.00, at fineness ratios of 3.0 and 5.0. The $n = 0.75$ body showed the lowest $C_{D,min}$ of any of the bodies tested, indicating the validity of the solutions for determining the minimum-drag shape.

Numerous experimental investigations performed on conical bodies at low supersonic speeds (ref. 4) and low-drag bodies of varying fineness ratio from low subsonic to hypersonic speeds (refs. 8 to 11) have indicated that large increases in $(L/D)_{max}$ are

obtainable by alteration of a circular-section body to an ellipse. For small values of ellipticity (2 or 3), only small reductions in volumetric efficiency $V^{2/3}/S_{wet}$ occur, with the result that increased performance may be obtained without excessive penalties in structural efficiency. If, therefore, advantage could be taken of minimum-pressure-drag bodies of elliptic rather than circular cross section, without large increases in the zero-lift pressure drag due to increased ellipticity, significant improvements in performance should result, as compared, for example, with a circular cone.

Suddath and Oehman (ref. 17) investigated this problem theoretically, using the method of analysis prescribed in reference 16; that is, $C_p = \frac{2(y')^2}{1 + (y')^2}$. Results of this investigation indicated that for the particular case of prescribed length and volume, no increase in the zero-lift pressure drag resulted from increasing ellipticity from 1 to approximately 4, and, further, for both the case of given length and volume and the case of given length and base height, the area distributions of the optimum body in question were insensitive to variations in ellipticity. Therefore, it became sufficient to calculate only the minimum-wave-drag body shape for an ellipse ratio of 1.0 (body of revolution), with the resultant area distributions permitting ordinates for ellipticities other than 1.0 to be obtained simply by setting the local ellipse cross-sectional area (πab) equal to the local circular cross-sectional area (πa^2). (Further discussion of this effect is included in the appendix of this paper.) Miele (ref. 21) explained the similarity of the longitudinal contours of circular and elliptic bodies, showing mathematically that the function which optimizes the longitudinal contour of an axisymmetric body is identical with the function which optimizes the longitudinal contour of any arbitrarily prescribed cross section. Results of these early investigations indicate that advantage can be taken of elliptic bodies for increasing performance at hypersonic speeds, without incurring large penalties in the zero-lift pressure drag.

Present Results

The bodies of the present investigation were designed under the geometric constraints of length and volume, which were constant for each body. The $n = 0.66$ body represents the minimum-wave-drag body (ref. 19) of the power-law bodies (volume and length constraint) and the $n = 1.00$ (conical) body represents the body of maximum lift (fig. 5) and minimum wetted area (fig. 1(b)). The body designated "Min-drag" in figure 1(b) is the shape determined under the exact solution derived by Eggers (ref. 16) and Suddath (ref. 17). The basic longitudinal aerodynamic characteristics of the bodies tested at $M = 10.03$ are presented in figures 4(a) to 4(f), and summary aerodynamic parameters for each body at $M = 10.03$ are presented in figure 5.

The effects of increasing power-body exponent on the longitudinal-aerodynamic parameters $C_{D,min}$, $(L/D)_{max}$, C_{L_α}, and x_{cp}/l for the circular and elliptic bodies, at a Mach number of 10.03 (fig. 5(a)), indicate that a minimum in the variation of $C_{D,min}$ with n occurs in the region of $n = 0.66$ for $a/b = 1.0$ and 2.0. As previously noted, this value of n represents the minimum-wave-drag body, if the stipulation is made that the shape must conform to a power relationship (ref. 19). The minimum-drag characteristics of the minimum-wave-drag bodies ($a/b = 1.0$ and 2.0), however, are somewhat lower than for the power bodies with $n = 0.66$. It is interesting to note that the longitudinal contour which gives the lowest value of $C_{D,min}$ is the same for either the circular or the elliptic cross-section body, thereby indicating experimental agreement with the similarity law derived by Miele in reference 21. The resultant $(L/D)_{max}$ characteristics indicate a maximum value at $n = 0.66$ for the power bodies, with the minimum-wave-drag body showing slightly higher values. It is interesting to note that compared with the conical bodies ($n = 1.00$), which have the highest C_{L_α} and minimum wetted area, a 25 to 30 percent increase in $(L/D)_{max}$ results from use of the $n = 0.66$ or minimum-wave-drag bodies, although their C_{L_α} values are only some 75 to 70 percent of the C_{L_α} values for the conical bodies. This effect illustrates the importance of minimizing the zero-lift pressure drag in improving the performance characteristics for lifting bodies of this type. The effect of increasing body exponent on the center of pressure at low angles of attack is shown in figure 5(a). A rearward shift in x_{cp}/l from approximately 0.53 for $n = 0.25$ to 0.67 for $n = 1.00$ is noted. The x_{cp}/l locations for each body conform approximately to the location of the centroid of planform area (ref. 11), as would be expected. Longitudinal center-of-pressure location for the minimum-wave-drag body is approximately 57 percent body length.

The effect of increasing ellipticity, for a given power body or the minimum-wave-drag body at $M = 10.03$ (fig. 5(a)), is a slight reduction in minimum-drag coefficient and an increase in C_{L_α} for each body (coefficients based on projected planform area). An almost constant incremental increase in $(L/D)_{max}$ is noted, independent of body longitudinal contour. These increases occur primarily as a result of the improved lift characteristics. This effect is better illustrated in figure 5(b), where $\left(\frac{L}{ql^2}\right)_\alpha$ and $\frac{D}{ql^2}$ are based on a common reference for each body ($l^2 = \text{const.}$). The large increases in lift-curve slope due to increased ellipticity more than offset the increases in minimum drag that result from the increased wetted area. It is interesting to note that there is little or no effect of ellipticity on the x_{cp}/l characteristics of a given body. A comparison of the volumetric and aerodynamic efficiency for the minimum-wave-drag body with $a/b = 2.0$ and the conic body of revolution indicates that, while $V^{2/3}/S_{wet}$ is

reduced by approximately 14 percent for the minimum-wave-drag body, an increase in $(L/D)_{max}$ of approximately 42 percent is realized.

Although the aerodynamic efficiency at hypersonic speeds is considerably greater for both the $n = 0.66$ and the minimum-wave-drag bodies than for a conical body of the same length and volume, the question arises as to possible off-design penalties which may occur at lower Mach numbers. Figure 6 presents a summary of the longitudinal aerodynamic parameters C_{L_α}, x_{cp}/l, $C_{D,min}$, and $(L/D)_{max}$ as functions of Mach number in the range from $M = 0.50$ to 10.03, for each body tested. The variations of $C'_{D,min}$ and $(L/D)'_{max}$ with Mach numbers from 1.5 to 10.03 are also included. Detailed discussion of pertinent results for a particular speed range may be found in reference 11 or 14. Although the $C_{D,min}$ and $(L/D)_{max}$ characteristics of the $n = 0.66$ body (optimum for the power bodies) and minimum-wave-drag body are approximately the same at hypersonic speeds (as noted in fig. 5), large reductions in $C_{D,min}$ and resultant increases in $(L/D)_{max}$ are noted for the minimum-wave-drag body as compared with the $n = 0.66$ body, especially near transonic and at subsonic speeds, when base-drag effects are included in total drag. These results tend to indicate that, because of the benefits realized at off-design conditions, the minimum-wave-drag body, rather than the body with $n = 0.66$, would offer additional benefits for an unpowered gliding-type vehicle.

Figures 6(d) and 6(f) present $C'_{D,min}$ and $(L/D)'_{max}$ for supersonic to hypersonic Mach numbers. As previously noted for the unadjusted base-drag results, $C'_{D,min}$ is as low for the minimum-wave-drag body as for any of the bodies tested ($a/b = 1.0$ or 2.0) and the resultant $(L/D)'_{max}$ values are generally as high as, or higher than, the values for the other bodies ($a/b = 1.0$ or 2.0), especially at the higher Mach numbers. It is interesting to note the relative insensitivity of $C'_{D,min}$ to increasing Mach number for the bodies with $n = 0.50$, 0.66, and 0.75 and the minimum-wave-drag bodies.

If these bodies are considered for use as fuselage forebodies, the minimum-wave-drag shape appears to offer both the lowest drag at the higher Mach numbers and the best base fairing because of the stipulation that $y' = 0$ at the base. The forward location of the longitudinal center of pressure, however, could introduce stability problems.

CONCLUDING REMARKS

An experimental investigation has been made at a Mach number of 10.03 to determine the longitudinal aerodynamic characteristics of a series of power-law bodies having values of the exponent of 0.25, 0.50, 0.66, 0.75, and 1.00, and a theoretical hypersonic minimum-wave-drag body. The bodies had the same length and volume, and the

theoretical body shape was determined under the geometric constraints of prescribed length and volume. For each body, cross-sectional shape was altered from circular to elliptic, while a constant longitudinal distribution of cross-sectional area was maintained. Results of the investigation may be summarized in the following observations.

For the series of power-law bodies tested, a minimum in the variation of zero-lift drag with body exponent occurs for an exponent of 0.66. A resultant maximum in the variation of maximum lift-drag ratio with body exponent also was found for an exponent of 0.66 for ellipse ratios of 1.0 and 2.0. The zero-lift drag characteristics of the theoretical hypersonic minimum-wave-drag body are slightly lower than those noted for the 0.66-power body, the maximum lift-drag-ratio characteristics being somewhat higher for ellipse ratios of 1.0 and 2.0.

The effects of increasing ellipticity for a given power-law body or the minimum-wave-drag body resulted in an almost constant incremental increase in maximum lift-drag ratio, independent of body longitudinal contour. These increases were primarily a result of the improved lift characteristics.

Langley Research Center,
National Aeronautics and Space Administration,
Langley Station, Hampton, Va., July 22, 1966,
126-13-03-03-23.

APPENDIX

PARAMETRIC STUDY OF THE SOLUTIONS OF THE HYPERSONIC MINIMUM-WAVE-DRAG BODY EQUATIONS FOR THE GIVEN LENGTH AND VOLUME CONSTRAINT

This appendix presents a systematic study of the solutions of the parametric equations of the minimum-wave-drag body shape and includes the effects of both fineness ratio and ellipticity for the imposed geometric constraints of fixed length and volume with the primary purpose of permitting the rapid, accurate determination of the minimum-wave-drag body ordinates through the use of simple design charts. The wetted area, planform area, and the corresponding wave drag for these bodies may also be determined from these charts.

Symbols

The symbols used in this appendix which differ from those used in the text are the following:

D_w	wave drag
F	fineness ratio, $l/2y_b$
y'	local body slope, dy/dx, $0 \leqq y' \leqq 1$
α	function defined by equation (A2)
η	function defined by equation (A4)
λ	nonpositive Lagrange multiplier
μ	ellipticity, major-to-minor axis ratio with the major axis horizontal, a/b

Subscripts:

0	at body nose
b	at body base
x	at any local longitudinal position on the body

APPENDIX

Discussion

The equations for the hypersonic minimum-wave-drag body shape having fixed length and volume are presented here with a brief discussion of the way in which they are used. These equations were originally derived in reference 16 for bodies of circular cross section and are derived in reference 17 for bodies of elliptic cross section. The derivation of these equations will not be repeated here. The equations are based on an exact Newtonian pressure law $\left(\text{that is, } C_p = \frac{2y'}{1 + (y')^2}\right)$. The following equations are taken from reference 17.

The lateral coordinate y of the local body cross section is found from

$$\lambda y = \alpha - \sqrt{\alpha^2 + (\lambda y_b)^2} \tag{A1}$$

where

$$\alpha = \frac{(y')^3\left[\frac{2}{\mu^2} + \left(1 + \frac{1}{\mu^2}\right)(y')^2\right]}{\left\{\left[1 + (y')^2\right]\left[\frac{1}{\mu^2} + (y')^2\right]\right\}^{3/2}} \tag{A2}$$

The integral for the longitudinal location x of a particular body section is

$$\lambda x = \int_{y_0'}^{y_x'} \eta \left[1 - \frac{\alpha}{\sqrt{\alpha^2 + (\lambda y_b)^2}}\right] dy' \tag{A3}$$

where

$$\eta = \frac{y'\left[\frac{6}{\mu^4} + \frac{5}{\mu^2}\left(1 + \frac{1}{\mu^2}\right)(y')^2 + 2\left(1 - \frac{1}{\mu^2} + \frac{1}{\mu^4}\right)(y')^4 - \left(1 + \frac{1}{\mu^2}\right)(y')^6\right]}{\left\{\left[1 + (y')^2\right]\left[\frac{1}{\mu^2} + (y')^2\right]\right\}^{5/2}} \tag{A4}$$

In order to satisfy the constraints of length and volume, the slopes at the nose and base are, respectively, $y_0' = 1$ and $y_b' = 0$. For a complete discussion of the boundary conditions, see reference 17.

The total length of the body l is obtained by integrating equation (A3) with $y_x' = y_b' = 0$, which yields λl.

APPENDIX

The integral for the volume of the body is

$$\lambda^3 V = \pi\mu \int_{y_0'}^{y_b'} \eta \left[\alpha - \sqrt{\alpha^2 + (\lambda y_b)^2}\right]^2 \left[1 - \frac{\alpha}{\sqrt{\alpha^2 + (\lambda y_b)^2}}\right] dy' \tag{A5}$$

The local cross-sectional area A_x is given by

$$\lambda^2 A_x = \pi\mu(\lambda y)^2 \tag{A6}$$

The value of the nonpositive Lagrange multiplier λ can be found by using the relation

$$\lambda = \frac{\lambda l}{l} \tag{A7}$$

since l is known.

In solving these equations for a specific length and volume, the composite parameter λy_b is adjusted until the parallel solution of equations (A3) and (A5) yields the specified values of length and volume. Equations (A3) and (A6) determine the body shape when solved using the particular value of λy_b. After the body ordinates are found, the wetted area, planform area, and wave drag can be computed.

The equation for the wetted area S_{wet} of the body is

$$S_{wet} = 4\mu \int_0^l y\sqrt{1 + (y')^2}\, E(\pi/2,k)\, dx \tag{A8}$$

where $E(\pi/2,k)$ is the complete elliptic integral of the second kind and k is defined by

$$k = \left[\frac{1 - \frac{1}{\mu^2}}{1 + (y')^2}\right]^{1/2}$$

The equation for the planform area S is

$$S = 2\mu \int_0^l y\, dx$$

APPENDIX

The wave drag D_w associated with the body is

$$D_w = 2\pi q\mu\left(y_0^2 + \int_0^l \frac{2y(y')^3}{\left\{\left[1 + (y')^2\right]\left[\frac{1}{\mu^2} + (y')^2\right]\right\}^{1/2}} dx\right) \tag{A9}$$

Results

Computer solutions of the theoretical minimum-wave-drag equations for given length and volume were generated which encompass a fineness-ratio range from 3 to 30. The normalized area distributions for three particular fineness ratios are shown in figures 7(a), 7(b), and 7(c). The result of this study is that the normalized longitudinal distribution of normalized local cross-sectional area (as weighted by body base area) is not significantly affected in the fineness-ratio range from 3 to 30, as shown in figure 7(d).

To dimensionalize the area distributions of figure 7, use the base area of the particular vehicle, as found from figure 8, and the length of the vehicle. The ordinates of the local body sections are then easily computed from the area equation of the chosen cross-sectional shape.

If additional accuracy is desired, the following procedure should be used. The equations may be integrated directly for the ordinates, once the values of λ and y_b are known. Previously, these quantities had to be determined by a tedious trial-and-error iteration procedure. The values of λ and y_b may be determined by using figures 9 and 10. For a specified V/l^3 ratio, the corresponding value of λy_b is given by figure 9; similarly, the value of λl is given by figure 10. Equation (A7) determines λ, and y_b can then be computed. The values of λ and y_b are used in integrating the equations for the body ordinates corresponding to the specified value of V/l^3.

The wetted areas for minimum-wave-drag bodies of several ellipticities are shown in nondimensional form in figure 11(a) and the planform areas are shown in figure 11(b). The wave-drag values associated with a series of circular bodies are shown in figure 12, also in nondimensional form. Wave-drag values were also computed for ellipticities μ of 2 and 3. These values are identical with those for the circular bodies shown in figure 12. The wetted-area and wave-drag information of these figures should prove useful in making total-drag estimates for proposed vehicles.

Figure 13 presents the relationship between the volume-to-length-cubed ratio and the equivalent fineness ratio for the minimum-wave-drag body. Also presented is the same relationship for a circular cone.

REFERENCES

1. Gregory, Thomas J.; Petersen, Richard H.; and Wyss, John A.: Performance Trade-Offs and Research Problems for Hypersonic Transports. AIAA Paper No. 64-605, Aug. 1964.

2. Baradell, Donald L.; and McLellan, Charles H.: Lateral-Range and Hypersonic Lift-Drag-Ratio Requirements for Efficient Ferry Service From a Near-Earth Manned Space Station. 2nd Manned Space Flight Meeting (Dallas, Texas), Am. Inst. Aeron. Astronaut., Apr. 1963, pp. 159-166.

3. Becker, John V.: Studies of High Lift/Drag Ratio Hypersonic Configurations. Proceedings of the 4th Congress of the International Council of the Aeronautical Sciences, Robert R. Dexter, ed., Spartan Books, Inc., 1965, pp. 877-910.

4. Jorgensen, Leland H.: Elliptic Cones Alone and With Wings at Supersonic Speeds. NASA Rept. 1376, 1958. (Supersedes NACA TN 4045.)

5. Carleton, W. E.; and Matthews, R. K.: The Aerodynamic Characteristics of Three Elliptical-Cone Lifting Bodies at Transonic Speeds. AEDC-TDR-63-53, U.S. Air Force, Apr. 1963.

6. Stivers, Louis S., Jr.; and Levy, Lionel L., Jr.: Longitudinal Force and Moment Data at Mach Numbers From 0.60 to 1.40 for a Family of Elliptic Cones With Various Semiapex Angles. NASA TN D-1149, 1961.

7. Fuller, Dennis E.; Shaw, David S.; and Wassum, Donald L.: Effect of Cross-Section Shape on the Aerodynamic Characteristics of Bodies at Mach Numbers From 2.50 to 4.63. NASA TN D-1620, 1963.

8. Spencer, Bernard, Jr.; and Phillips, W. Pelham: Effects of Cross-Section Shape on the Low-Speed Aerodynamic Characteristics of a Low-Wave-Drag Hypersonic Body. NASA TN D-1963, 1963.

9. Spencer, Bernard, Jr.; Phillips, W. Pelham; and Fournier, Roger H.: Supersonic Aerodynamic Characteristics of a Series of Bodies Having Variations in Fineness Ratio and Cross-Section Ellipticity. NASA TN D-2389, 1964.

10. Spencer, Bernard, Jr.; and Phillips, W. Pelham: Transonic Aerodynamic Characteristics of a Series of Bodies Having Variations in Fineness Ratio and Cross-Sectional Ellipticity. NASA TN D-2622, 1965.

11. Spencer, Bernard, Jr.: Transonic Aerodynamic Characteristics of a Series of Related Bodies With Cross-Sectional Ellipticity. NASA TN D-3203, 1966.

12. Fetterman, David E.; Henderson, Arthur, Jr.; Bertram, Mitchel H.; and Johnston, Patrick J.: Studies Relating to the Attainment of High Lift-Drag Ratios at Hypersonic Speeds. NASA TN D-2956, 1965.

13. Penland, Jim A.: Aerodynamic Force Characteristics of a Series of Lifting Cone and Cone-Cylinder Configurations at a Mach Number of 6.83 and Angles of Attack up to 130^{o}. NASA TN D-840, 1961.

14. Fournier, Roger H.; Spencer, Bernard, Jr.; and Corlett, William A.: Supersonic Aerodynamic Characteristics of a Series of Related Bodies With Cross-Sectional Ellipticity. NASA TN D-3539, 1966.

15. Foster, A. D., compiler: A Compilation of Longitudinal Aerodynamic Characteristics Including Pressure Information for Sharp- and Blunt-Nose Cones Having Flat and Modified Bases. SC-R-64-1311, Sandia Corp., Jan. 1965.

16. Eggers, A. J., Jr.; Resnikoff, Meyer M.; and Dennis, David H.: Bodies of Revolution Having Minimum Drag at High Supersonic Airspeeds. NACA Rept. 1306, 1957. (Supersedes NACA TN 3666.)

17. Suddath, Jerrold H.; and Oehman, Waldo I.: Minimum Drag Bodies With Cross-Sectional Ellipticity. NASA TN D-2432, 1964.

18. Miele, Angelo: Slender Shapes of Minimum Drag in Newtonian Flow. Z. Flugwissenschaften, Jahrg. 11, Heft 5, May 1963, pp. 203-210.

19. Lusty, Arthur H., Jr.: Slender, Axisymmetric Power Bodies Having Minimum Zero-Lift Drag in Hypersonic Flow. D1-82-0275, Flight Sci. Lab., Boeing Sci. Res. Lab., July 1963.

20. Putman, Lawrence E.; and Brooks, Cuyler W., Jr.: Static Longitudinal Aerodynamic Characteristics at a Mach Number of 10.03 of Low-Aspect-Ratio Wing-Body Configurations Suitable for Reentry. NASA TM X-733, 1962.

21. Miele, Angelo: Similarity Laws for Optimum Hypersonic Bodies. Astronautica Acta, vol. II, no. 3, 1965, pp. 202-206.

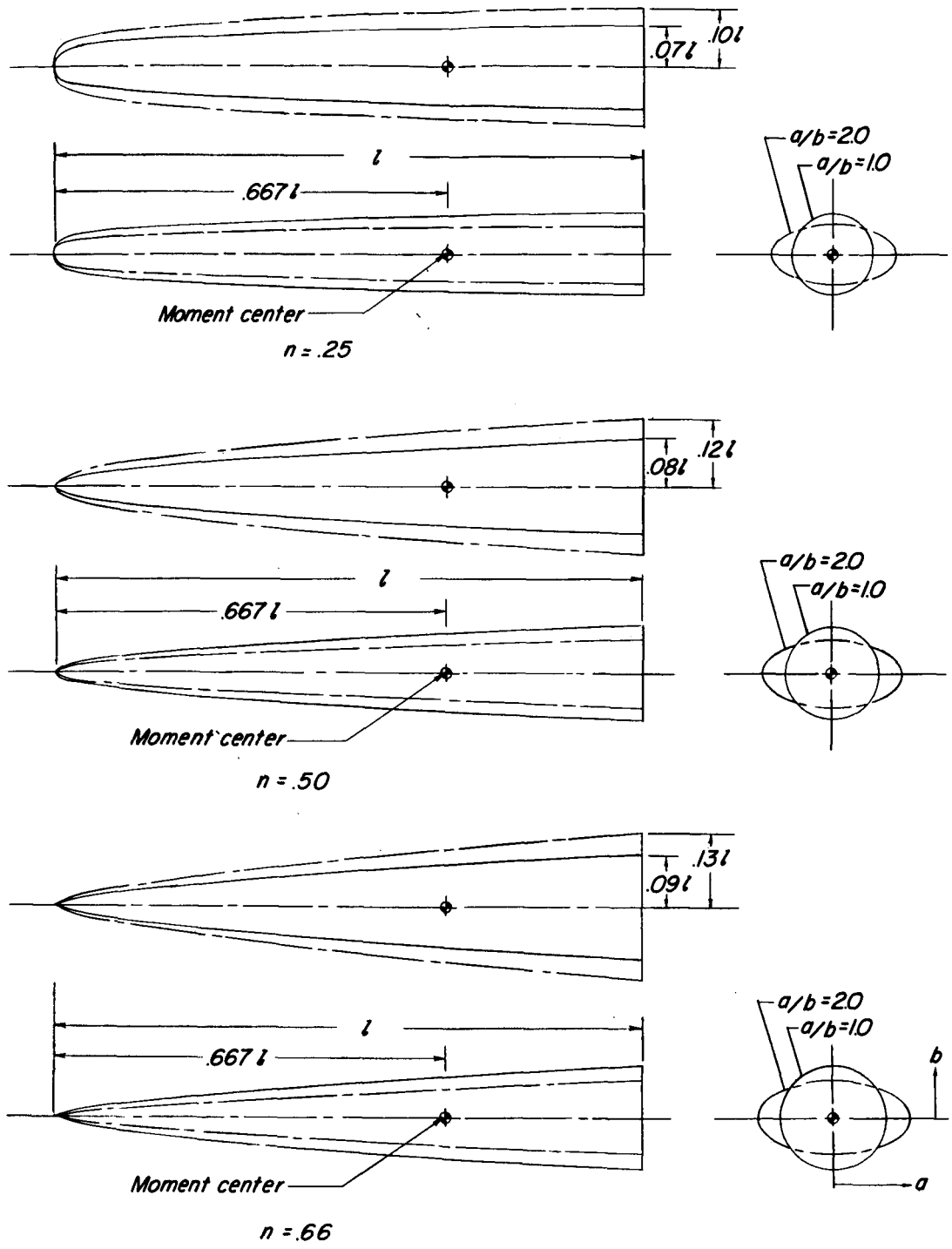

(a) Model drawings.

Figure 1.- Drawings and geometric characteristics of the various models tested.

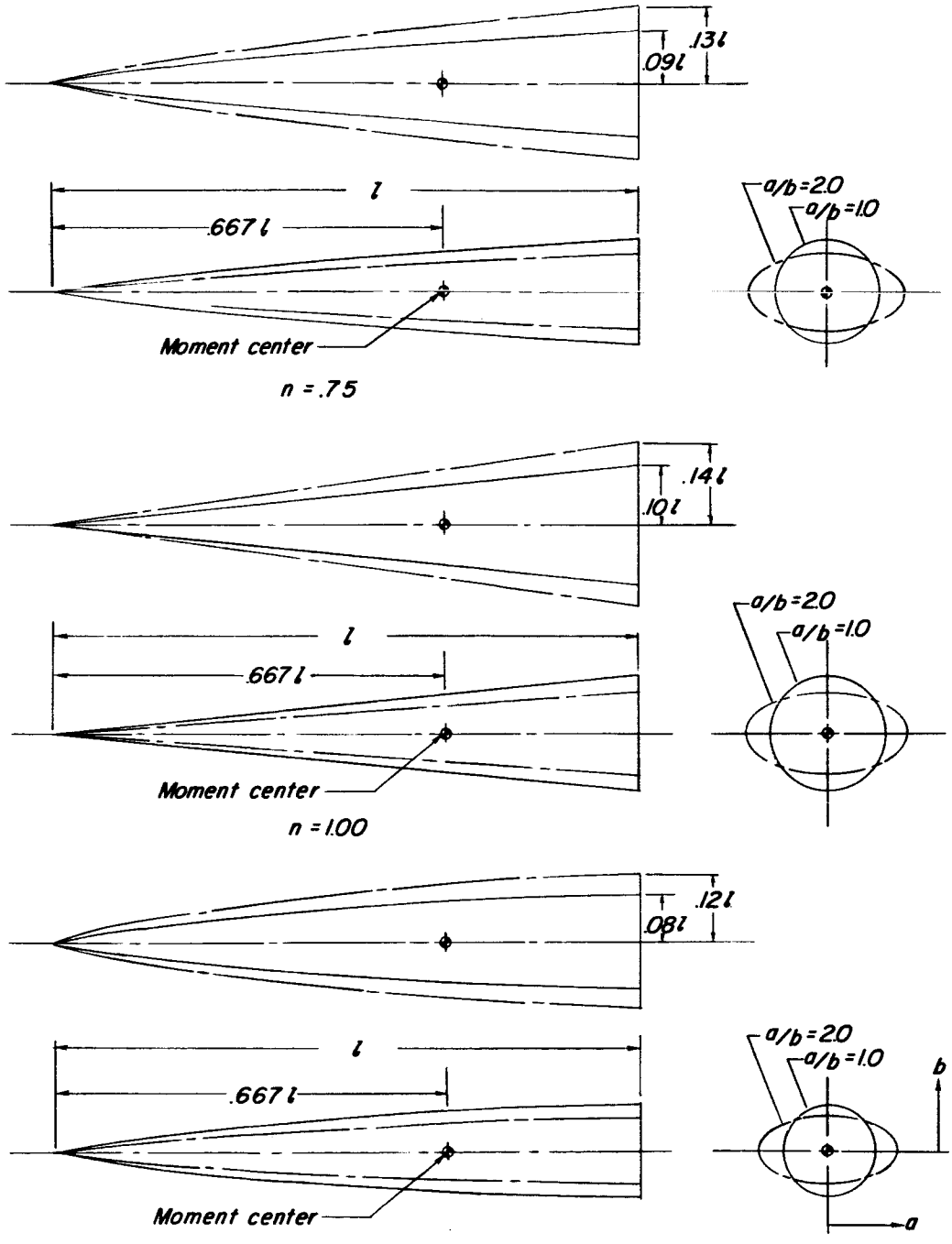

(a) Concluded.

Figure 1.- Continued.

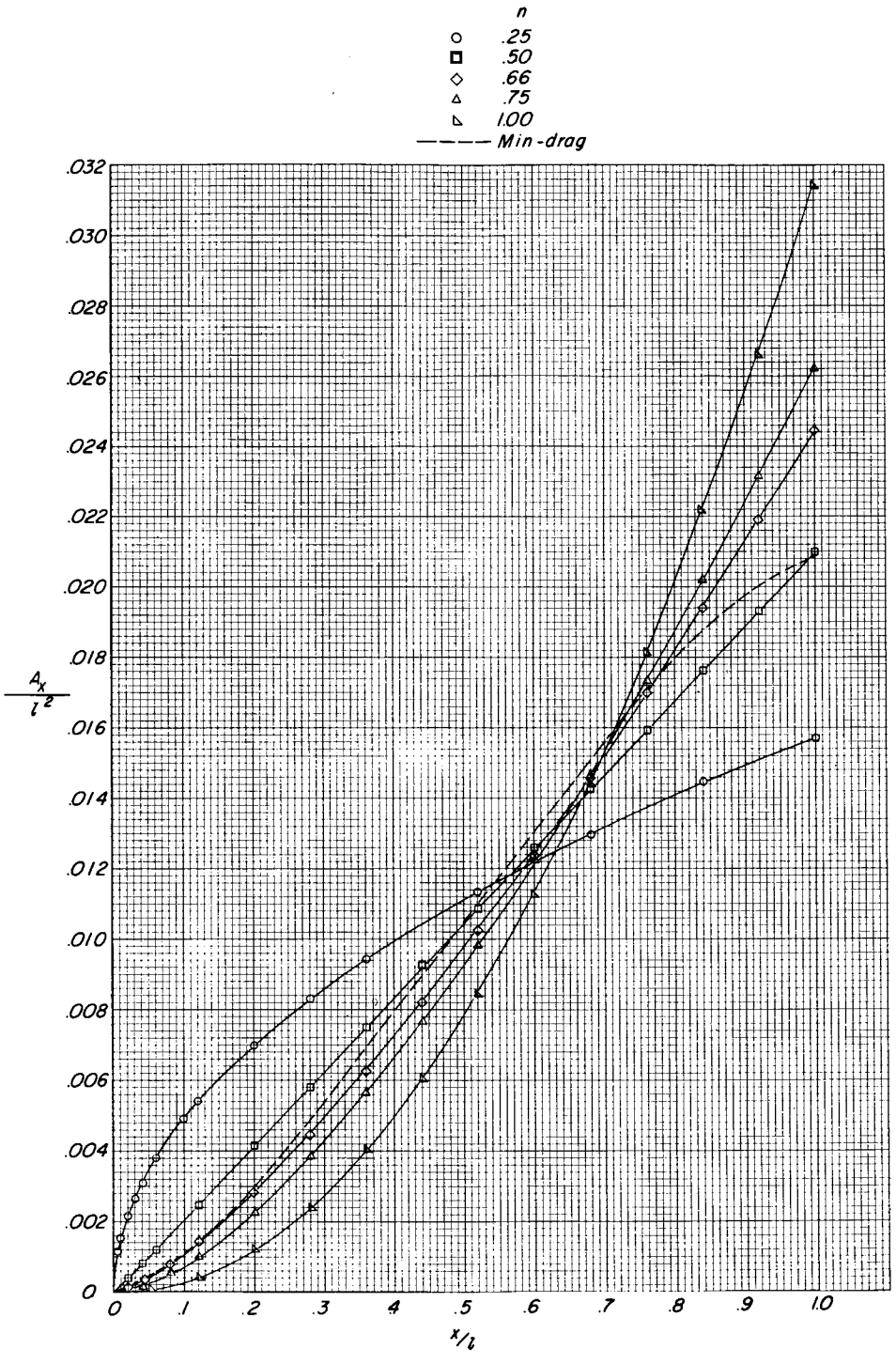

(b) Geometric characteristics.

Figure 1.- Continued.

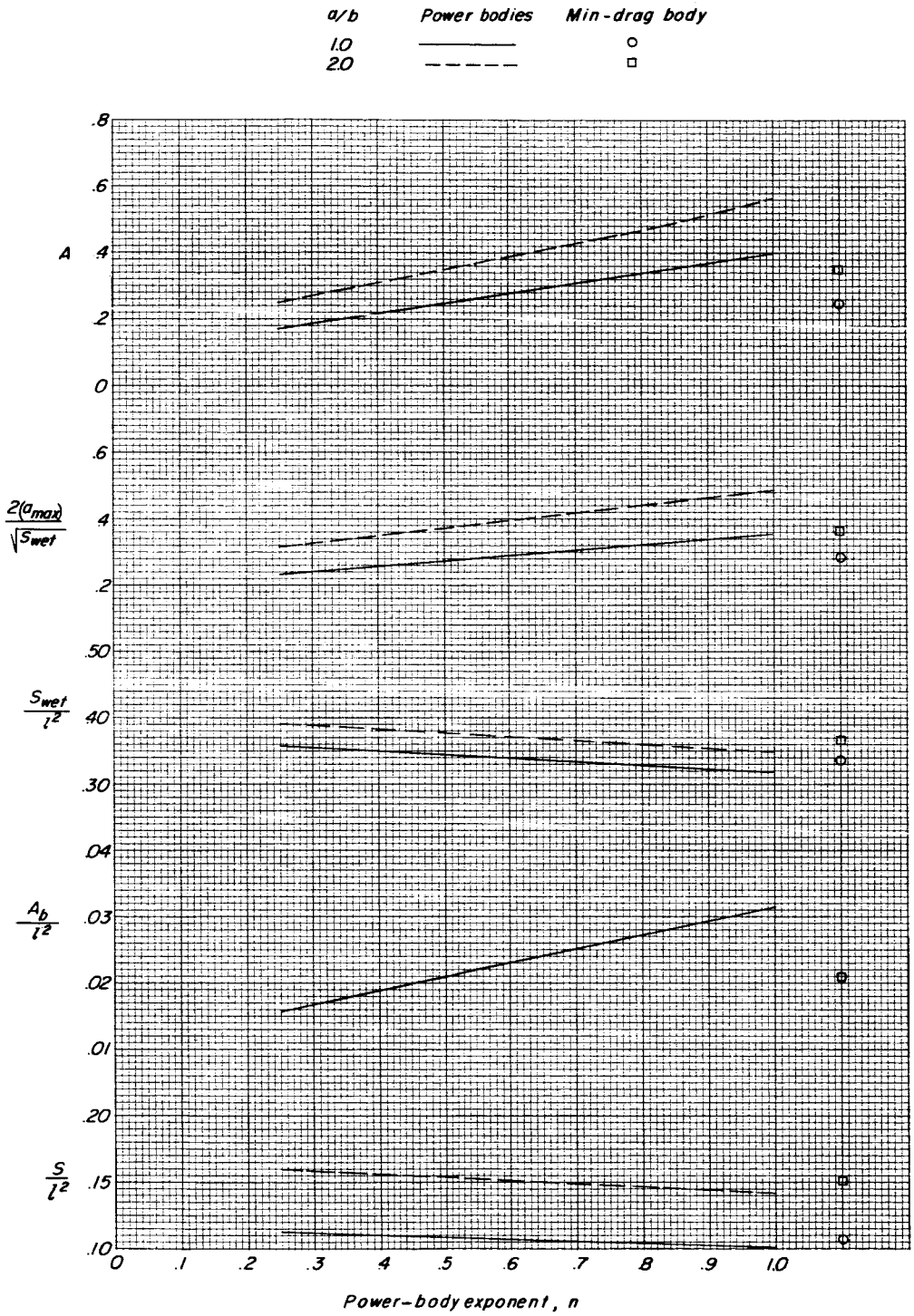

(b) Concluded.

Figure 1.- Concluded.

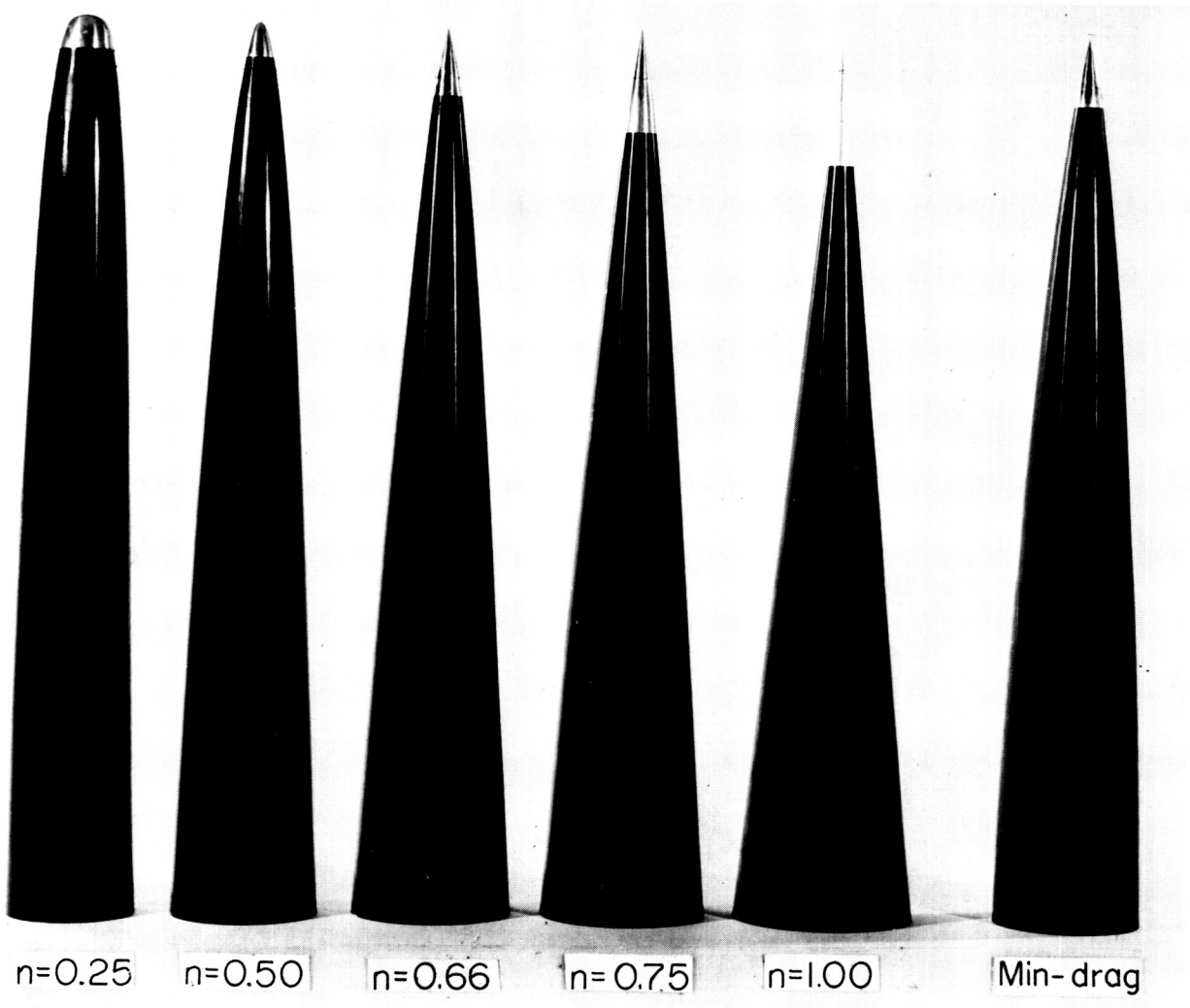

(a) a/b = 1.0.

L-65-2660

Figure 2.- Photographs of models.

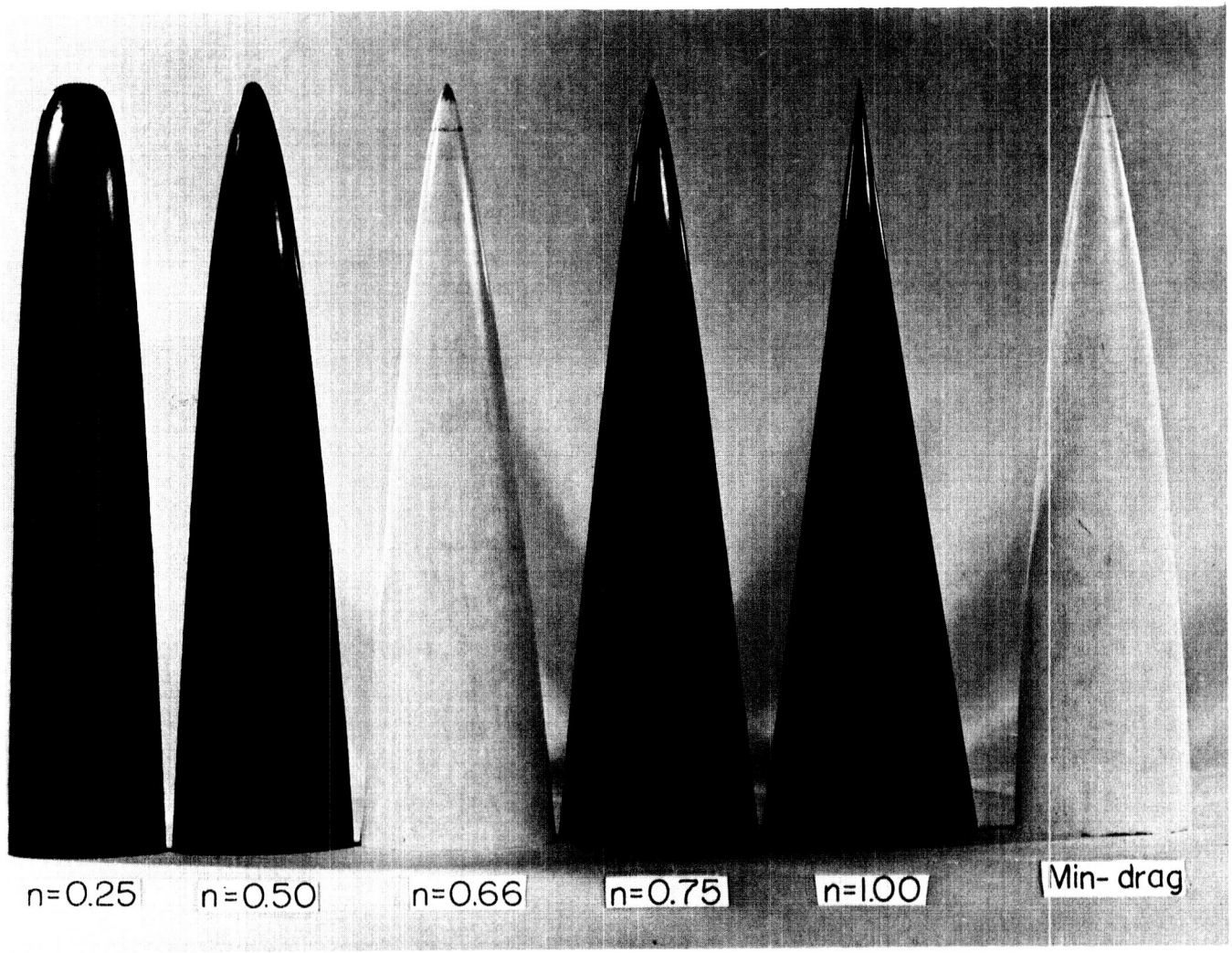

(b) a/b = 2.0. L-65-2658

Figure 2.- Concluded.

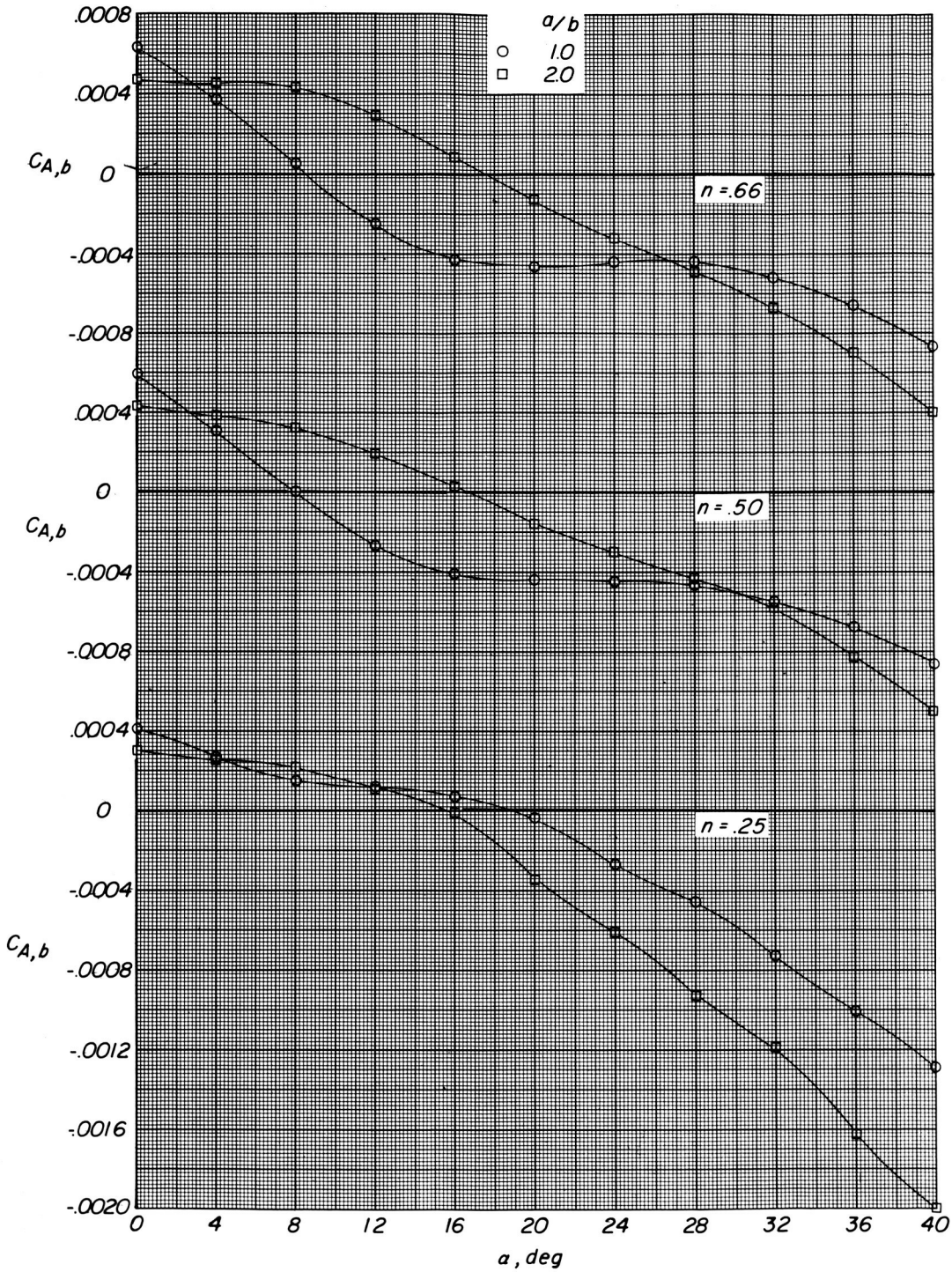

(a) Bodies with power-law exponents n = 0.25, 0.50, and 0.66.

Figure 3.- Variation of base axial-force coefficient with angle of attack for circular and elliptic bodies.

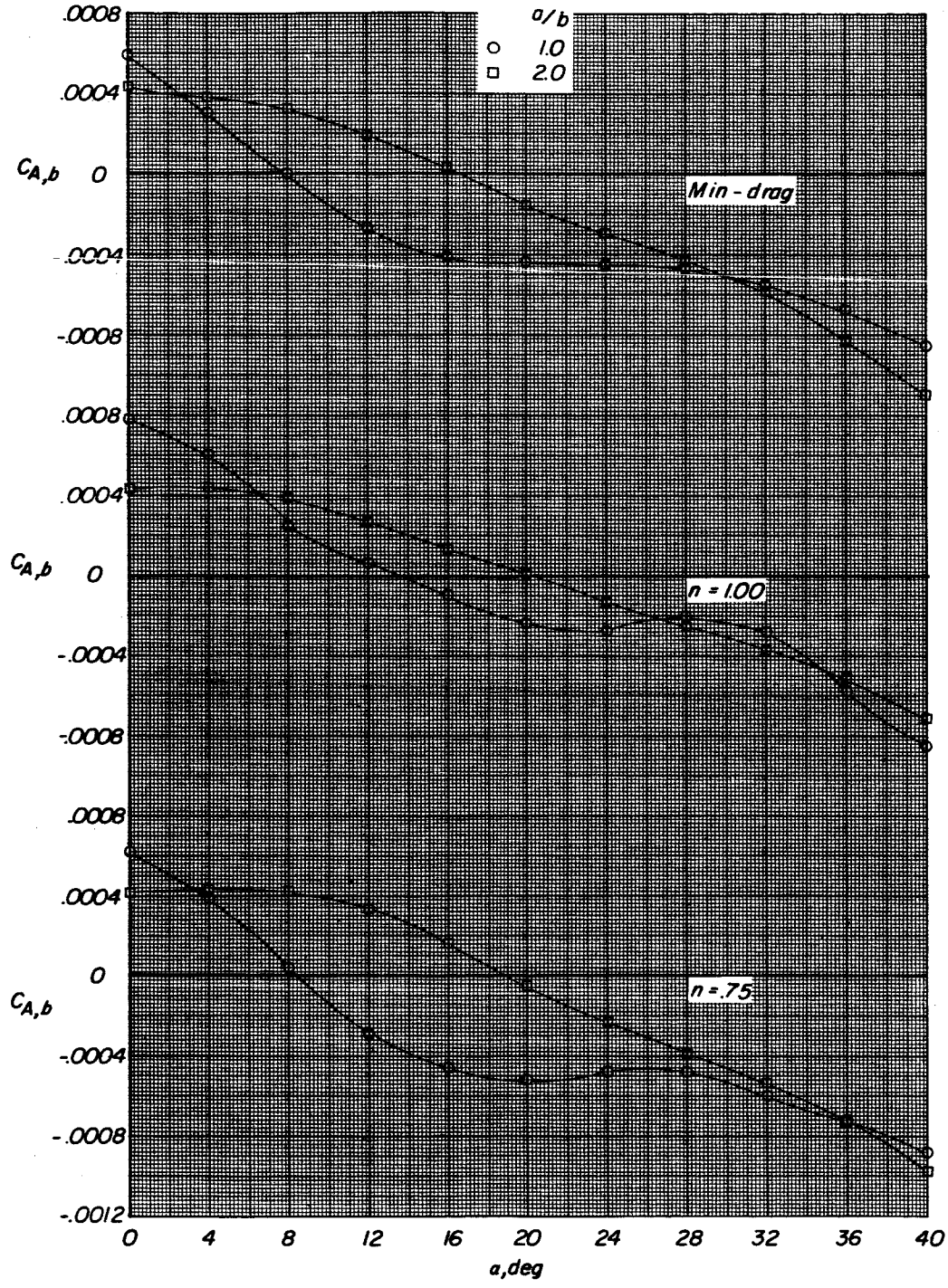

(b) Bodies with power-law exponent n = 0.75 and 1.00 and minimum-wave-drag body.

Figure 3.- Concluded.

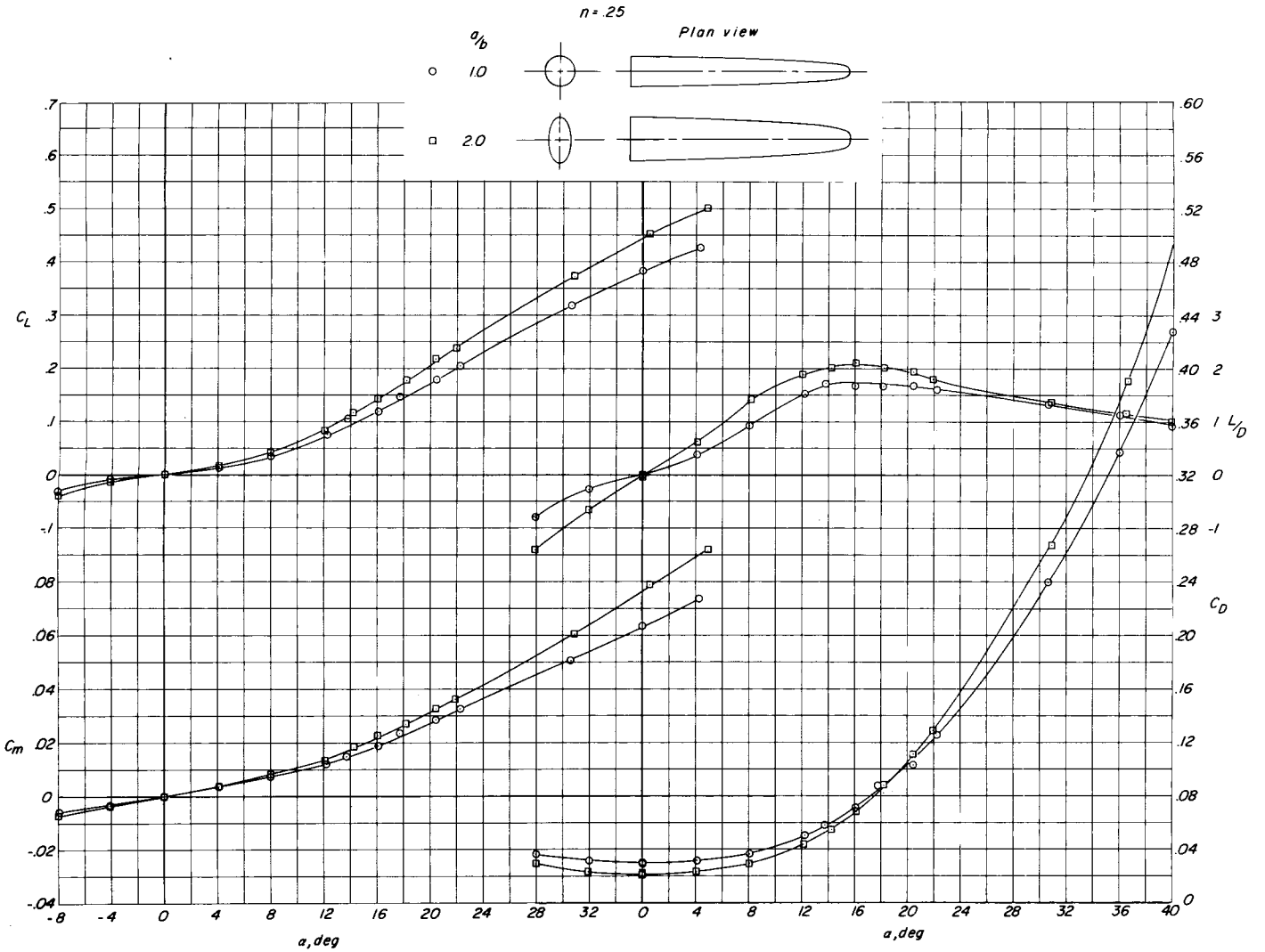

(a) n = 0.25.

Figure 4.- Longitudinal aerodynamic characteristics of series of power-law bodies and theoretical minimum-wave-drag bodies at a Mach number of 10.03.

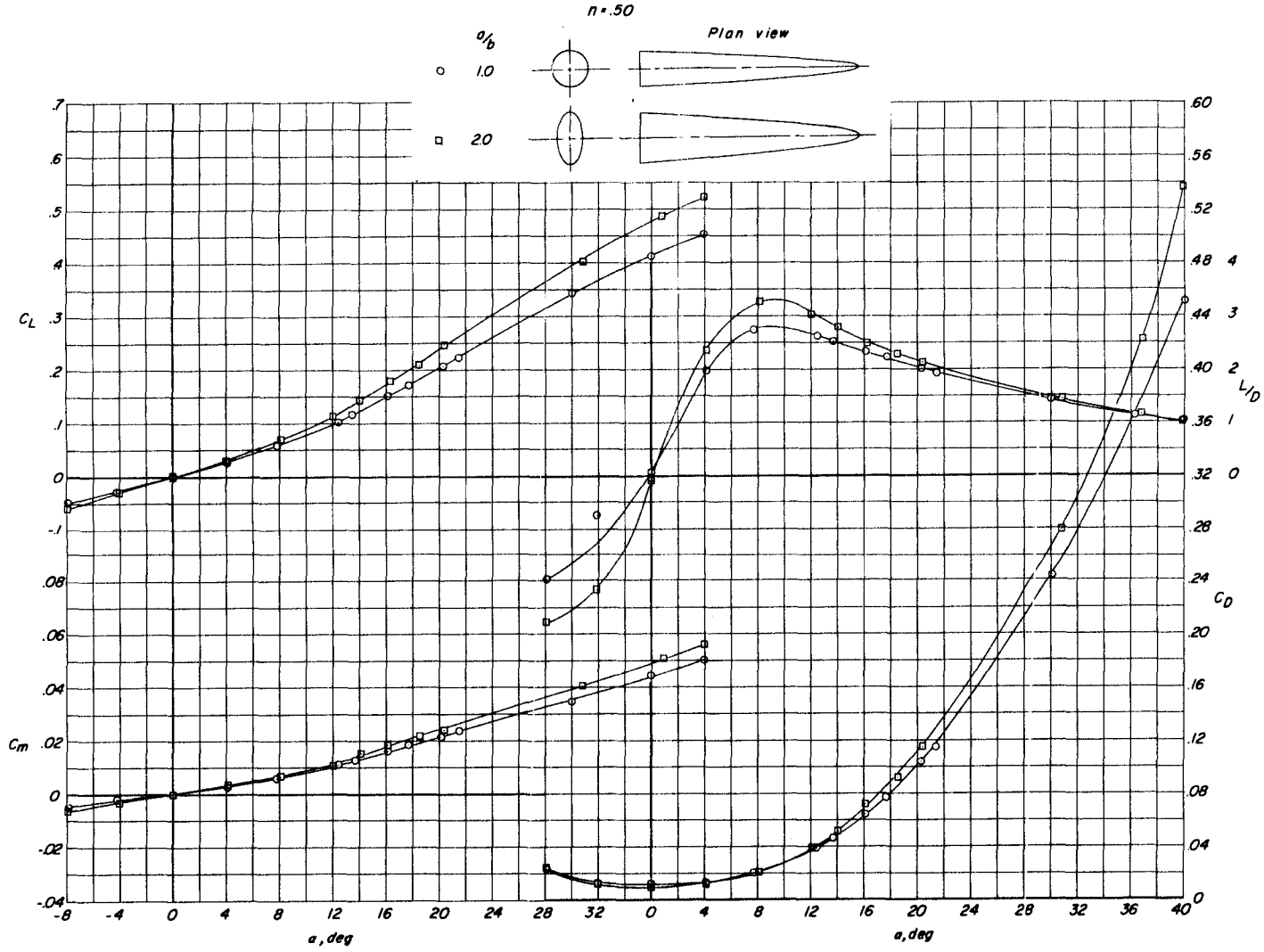

(b) n = 0.50.

Figure 4.- Continued.

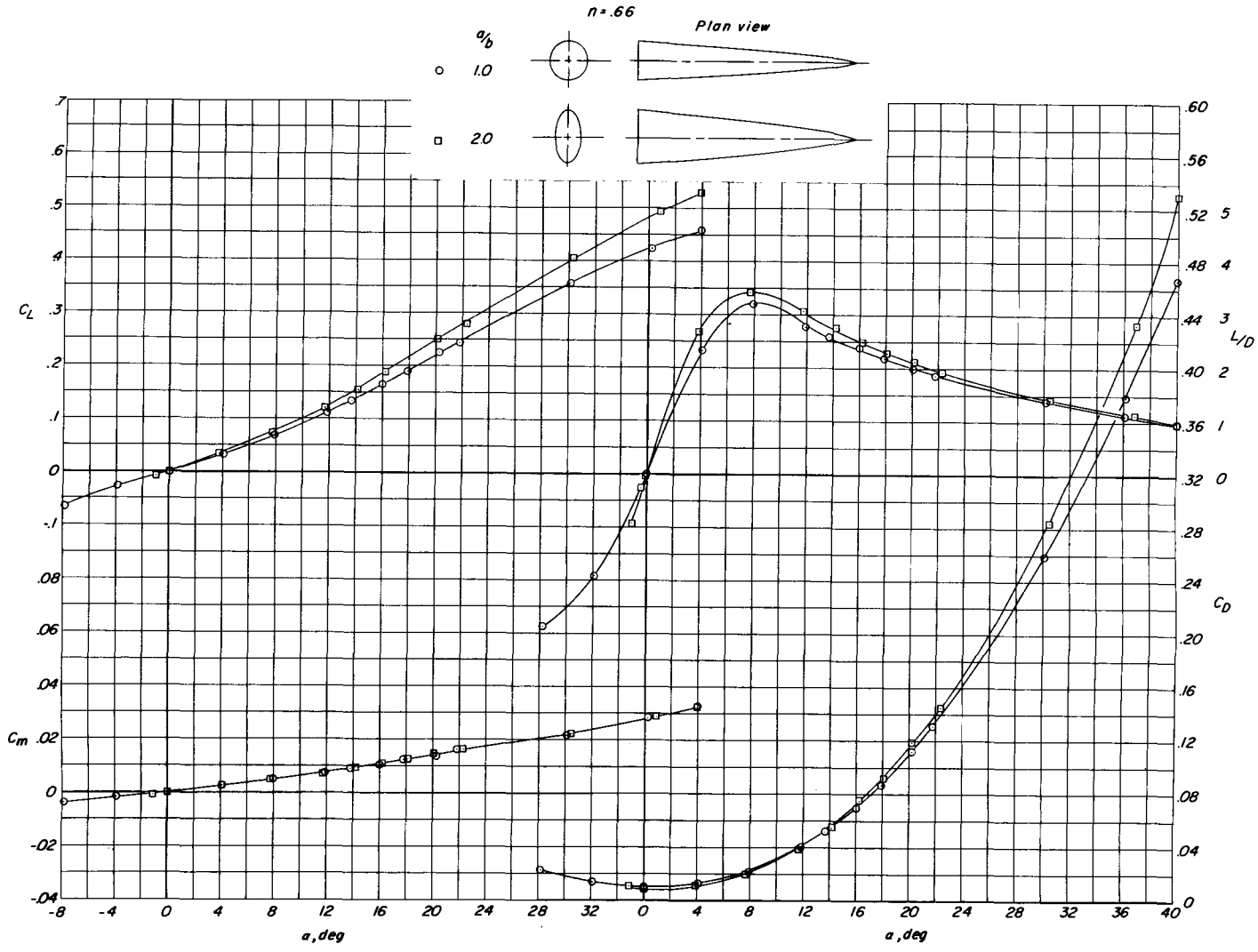

(c) n = 0.66.

Figure 4.- Continued.

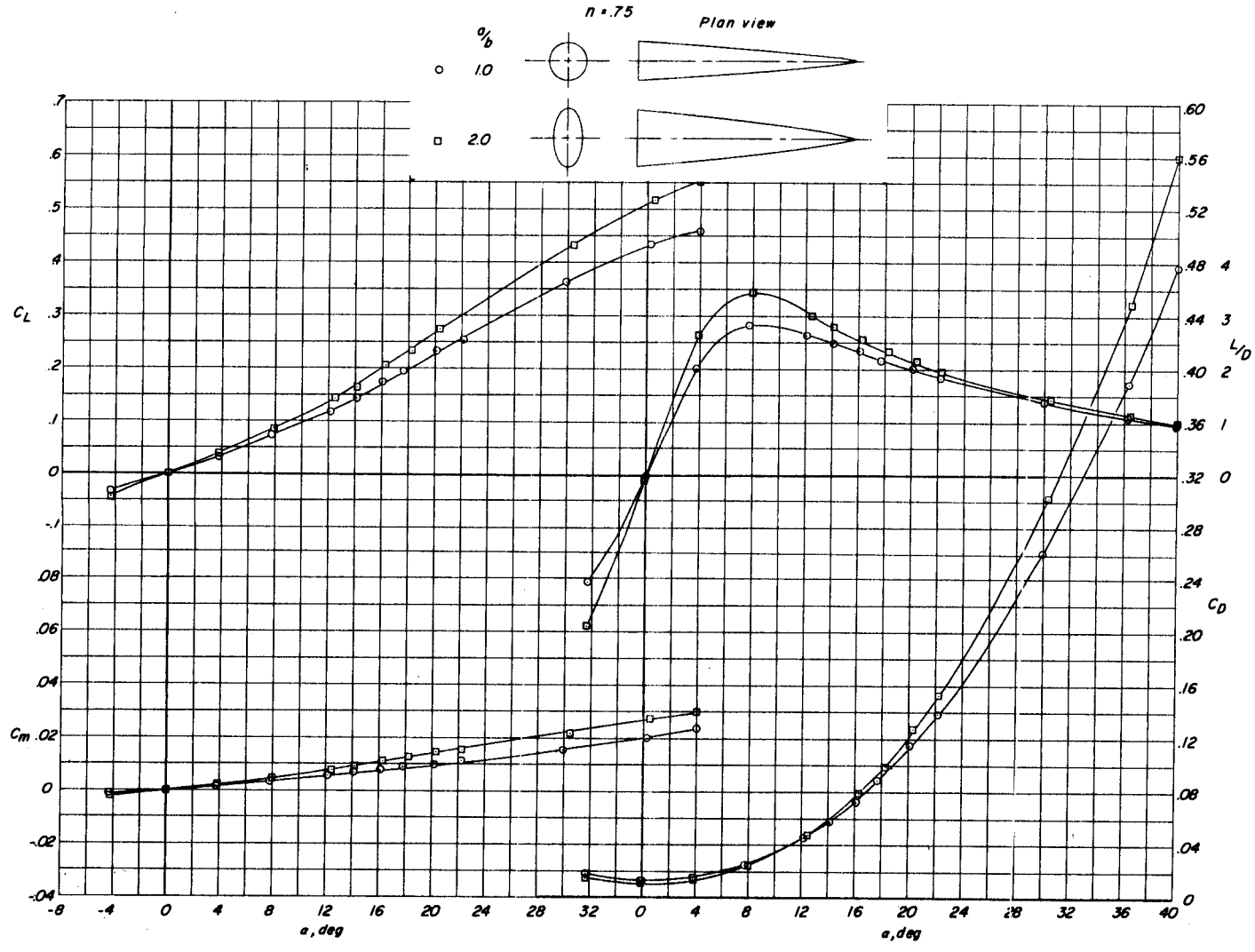

(d) n = 0.75.

Figure 4.- Continued.

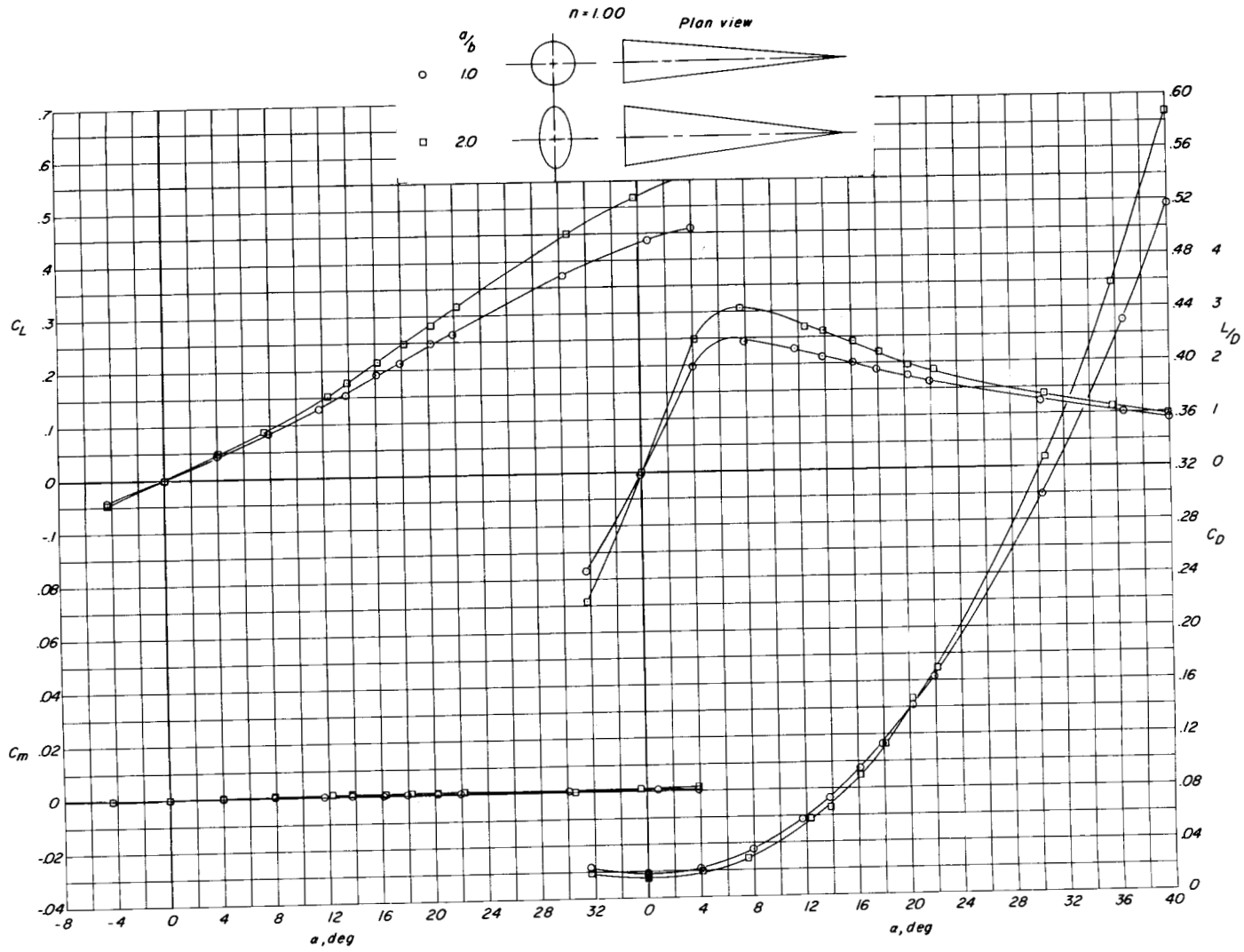

(e) n = 1.00.

Figure 4.- Continued.

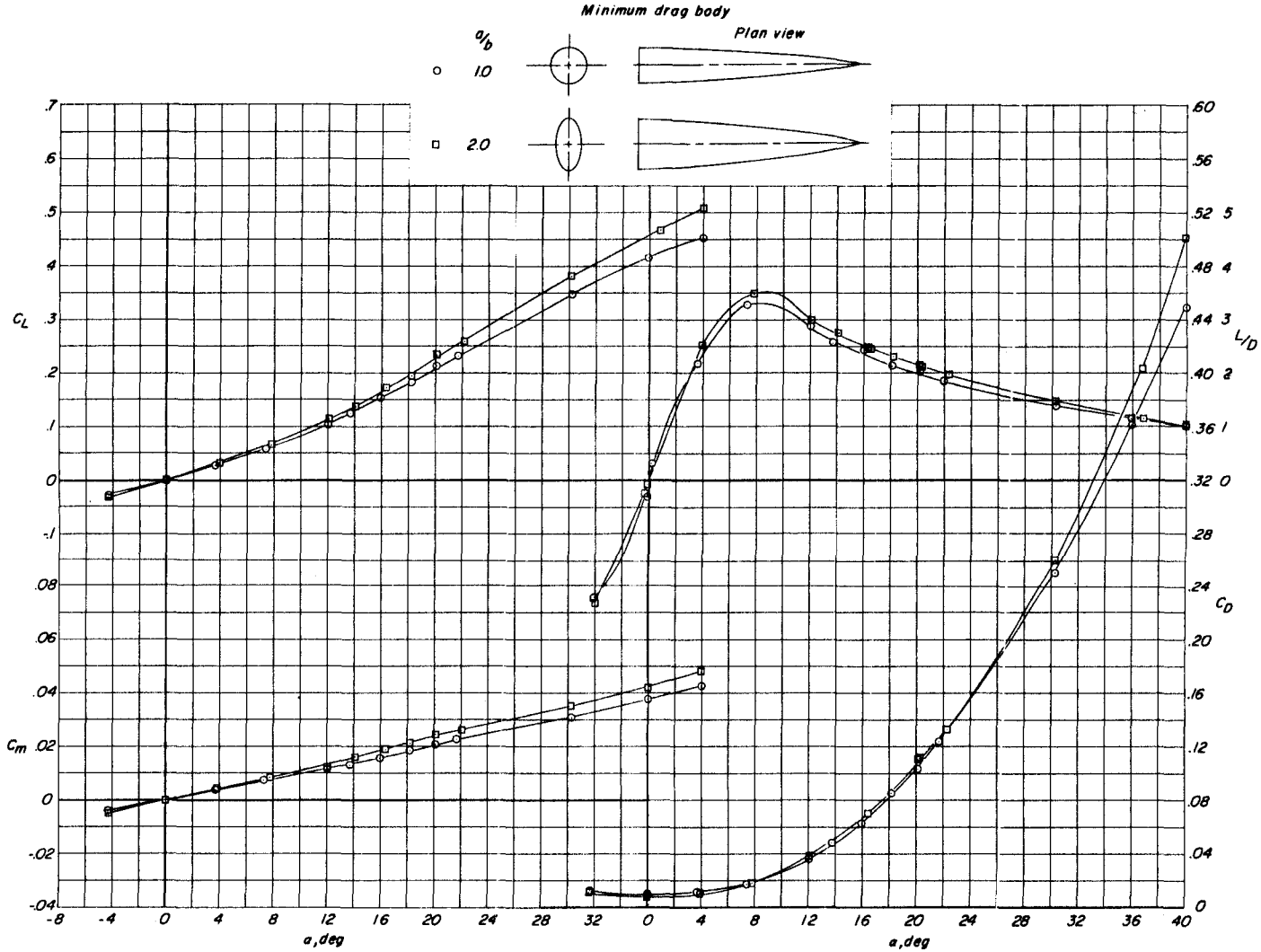

(f) Minimum-wave-drag body.

Figure 4.- Concluded.

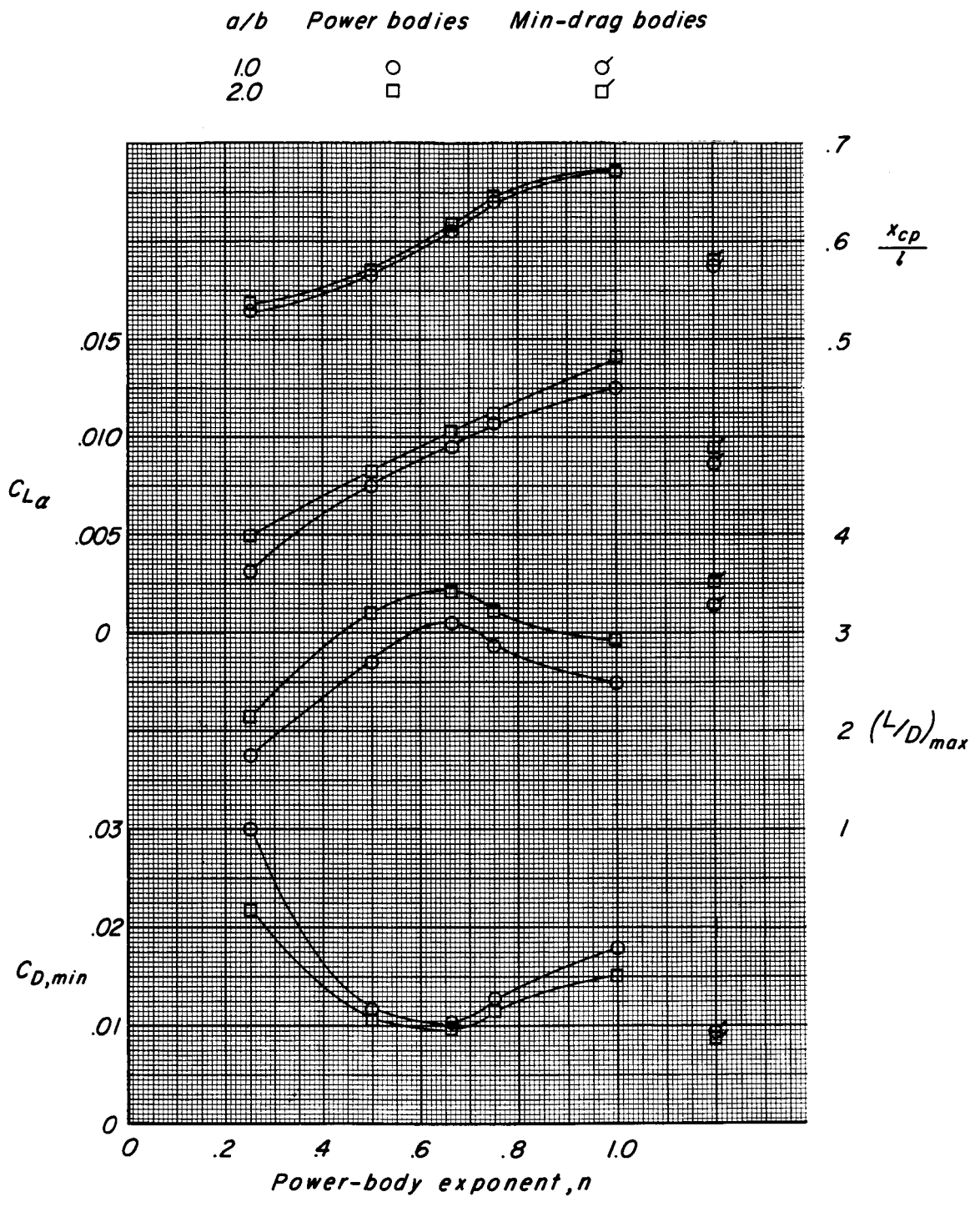

(a) Variation of C_{L_α}, x_{cp}/l, $(L/D)_{max}$, and $C_{D,min}$ with body exponent.

Figure 5.- Summary of longitudinal aerodynamic characteristics of series of power-law bodies and minimum-wave-drag body. M = 10.03.

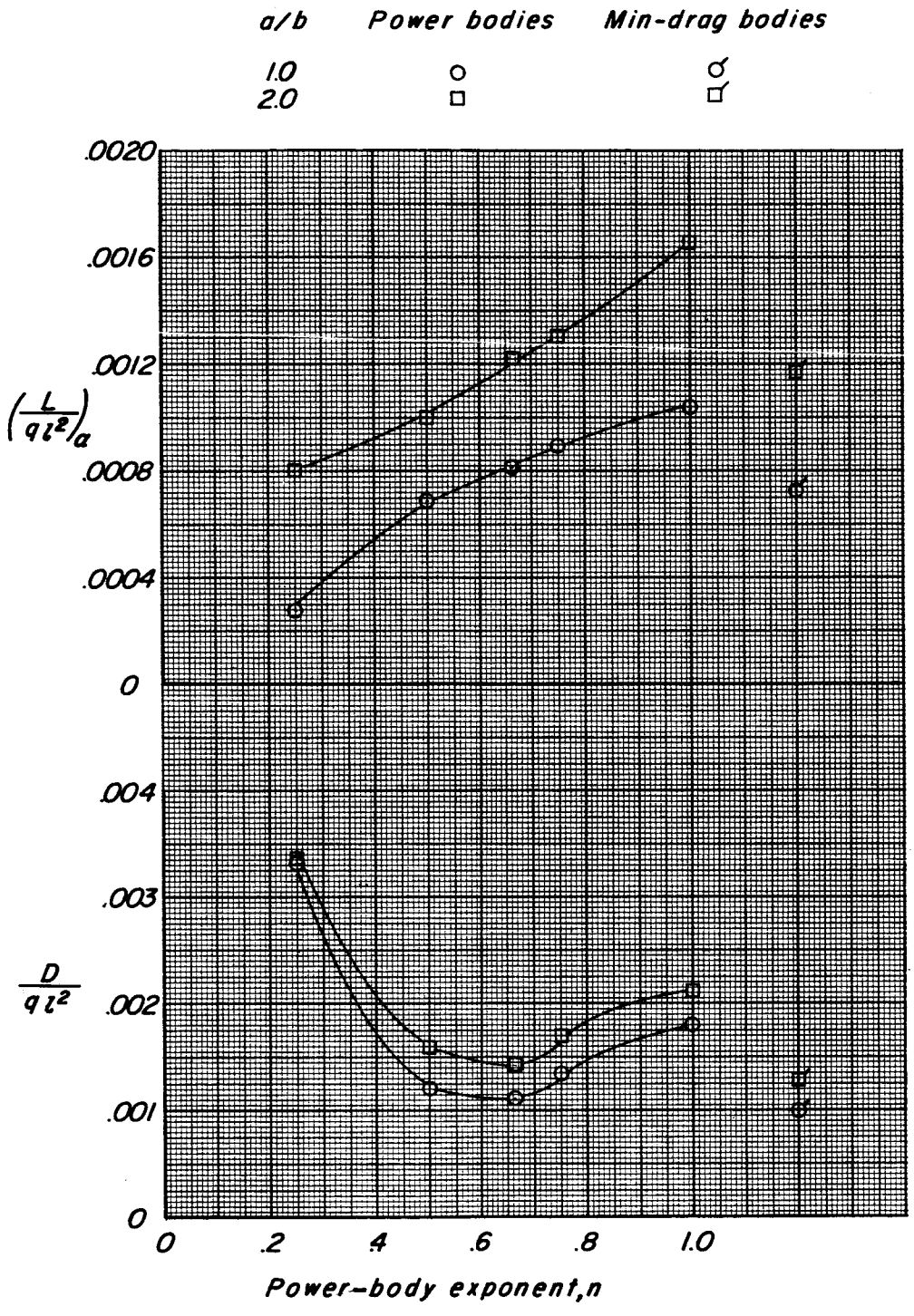

(b) Variation of $\left(\frac{L}{ql^2}\right)_a$ and $\frac{D}{ql^2}$ with body exponent. Length l is constant.

Figure 5.- Concluded.

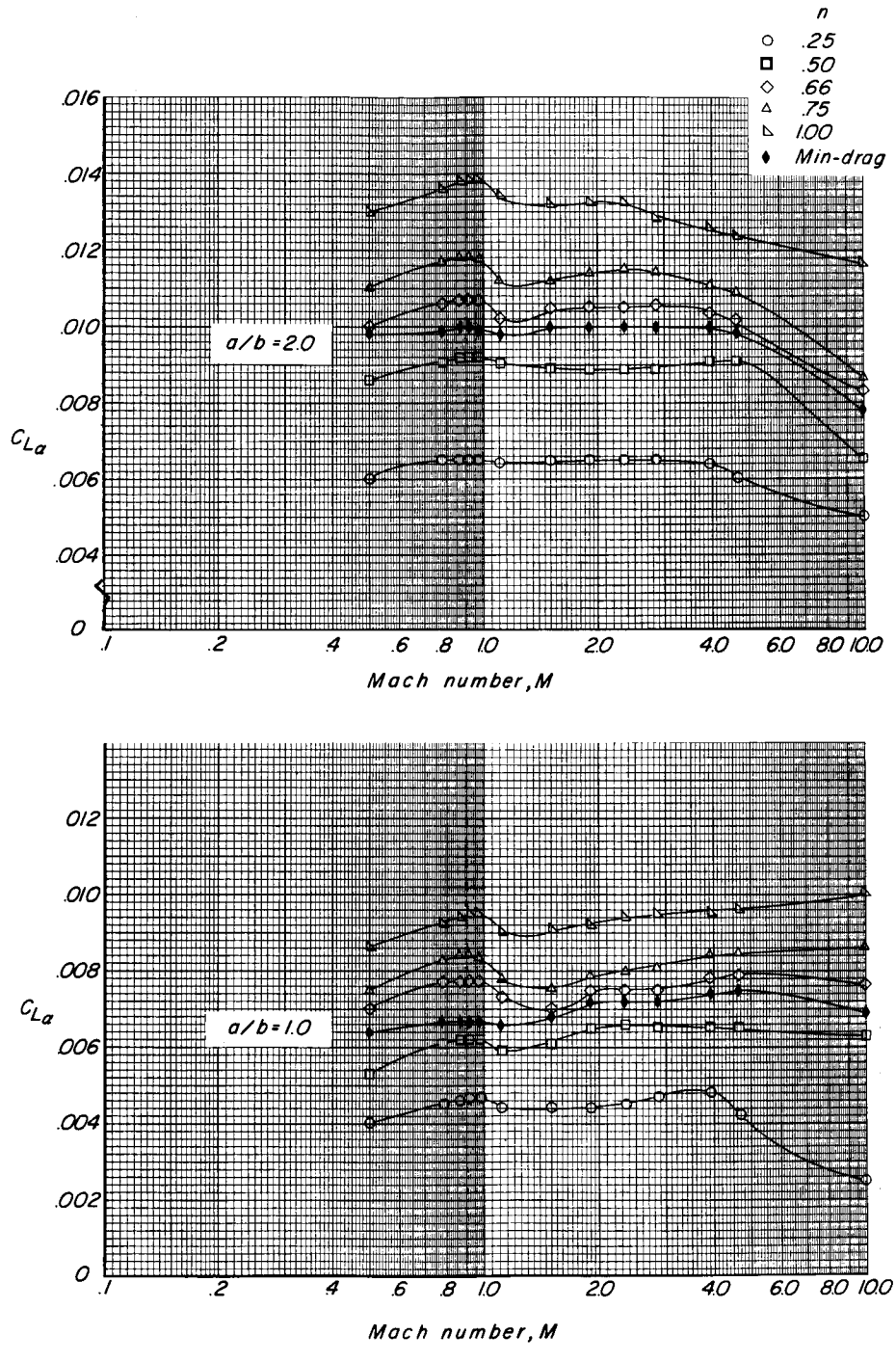

(a) Variation of C_{L_α} with Mach number.

Figure 6.- Summary of longitudinal aerodynamic parameters C_{L_α}, x_{cp}/l, $C_{D,min}$, $C'_{D,min}$, $(L/D)_{max}$, and $(L/D)'_{max}$ for power-law and minimum-wave-drag bodies, as functions of Mach number.

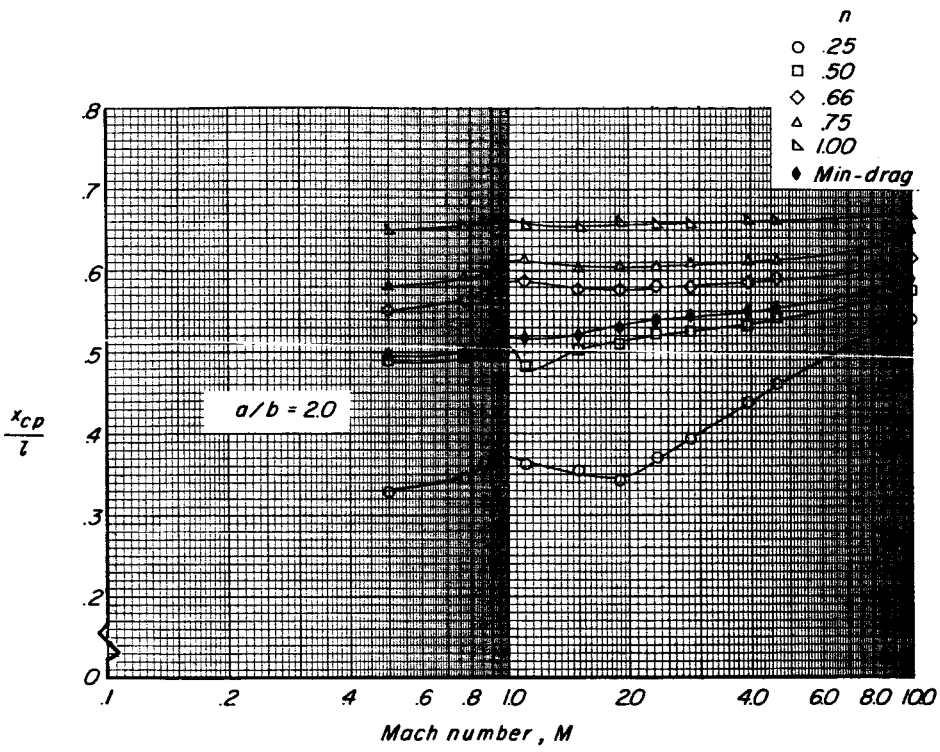

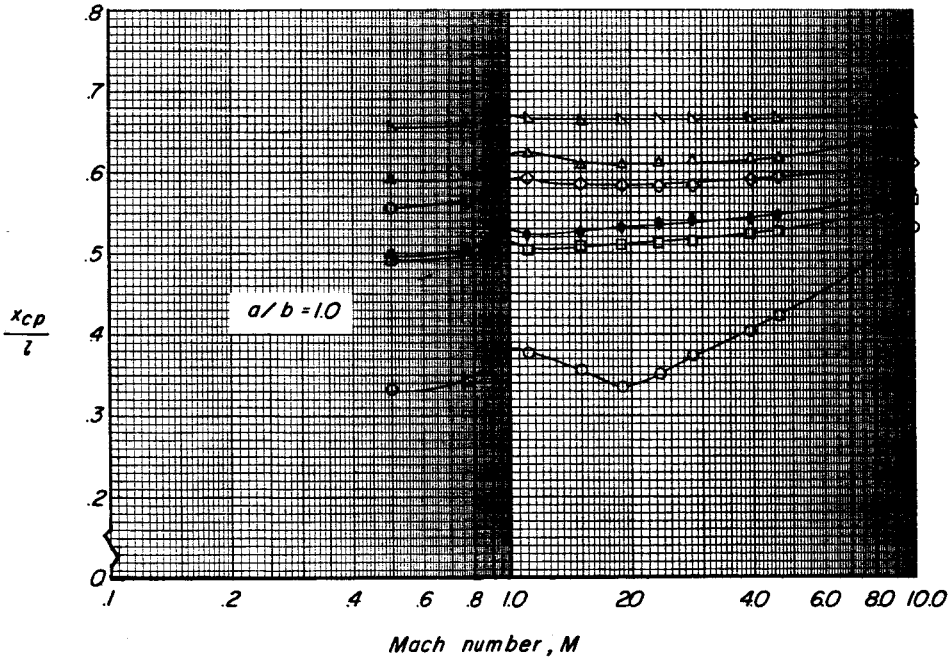

(b) Variation of x_{cp}/l with Mach number.

Figure 6.- Continued.

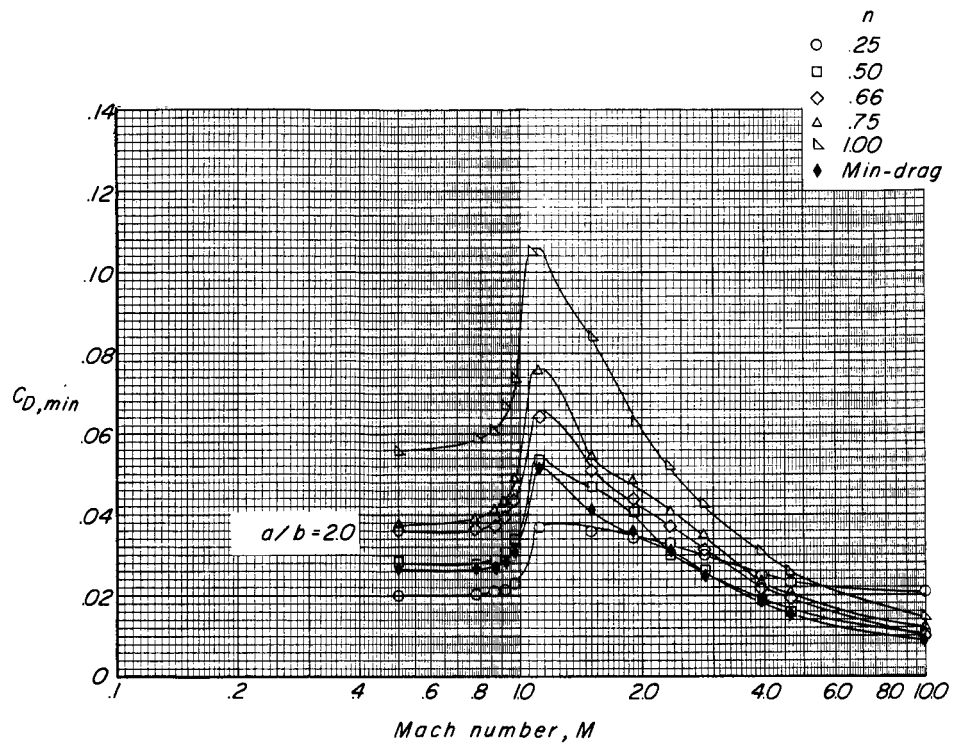

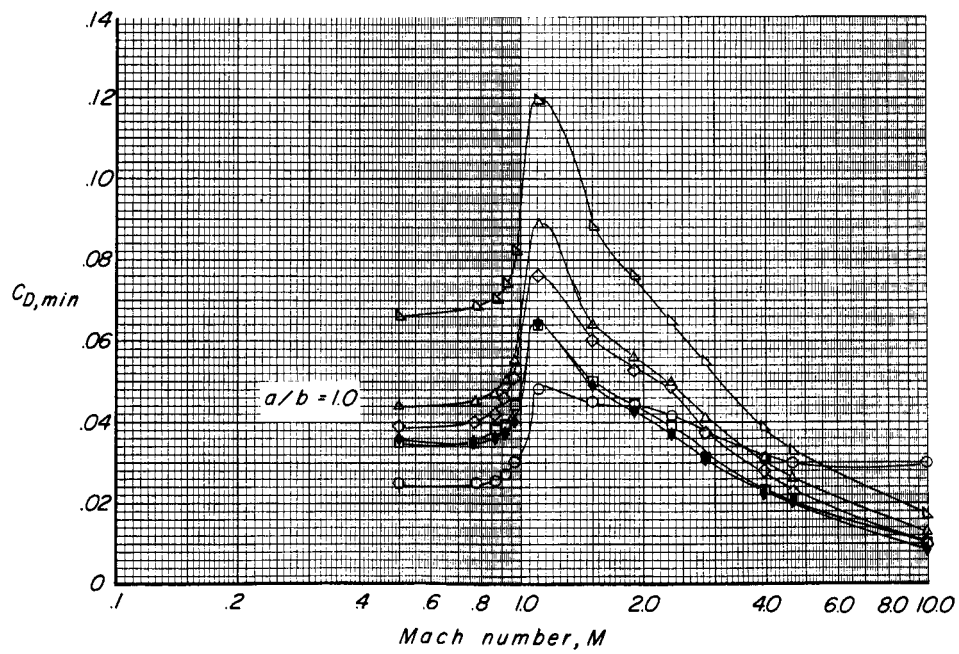

(c) Variation of $C_{D,min}$ with Mach number.

Figure 6.- Continued.

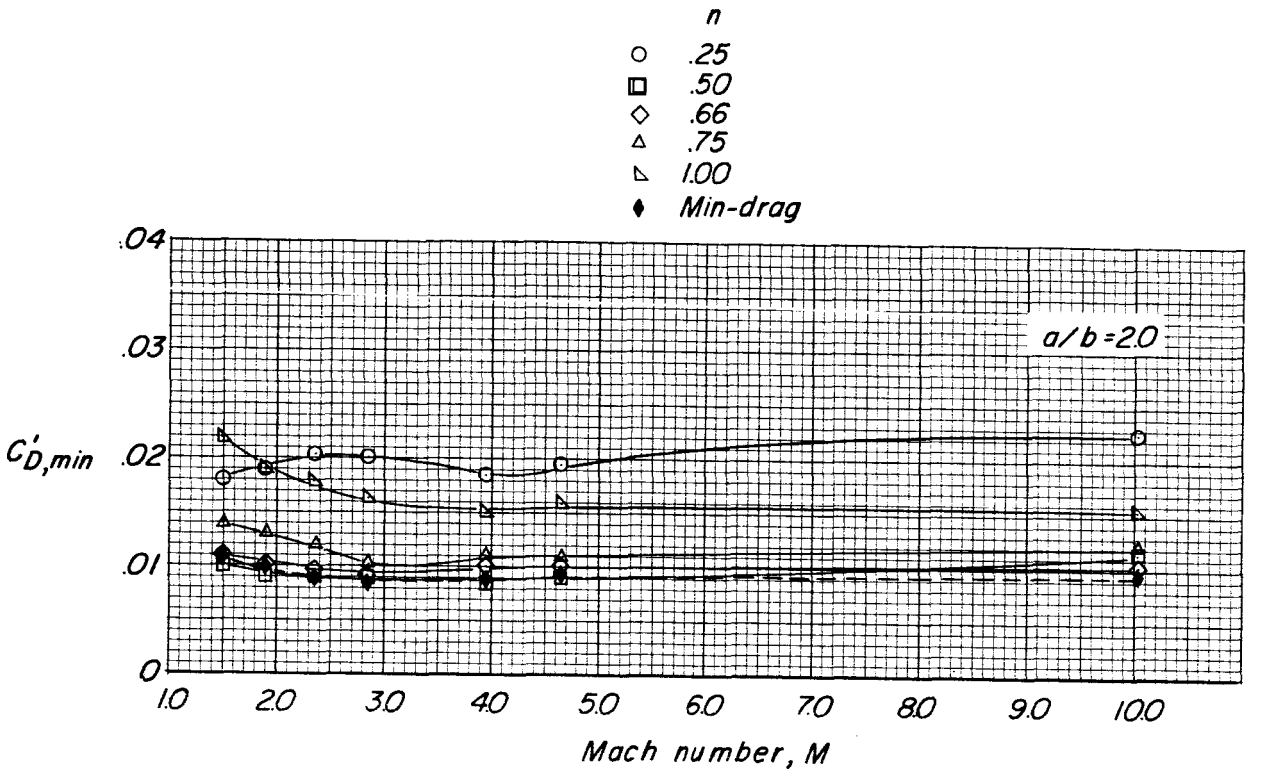

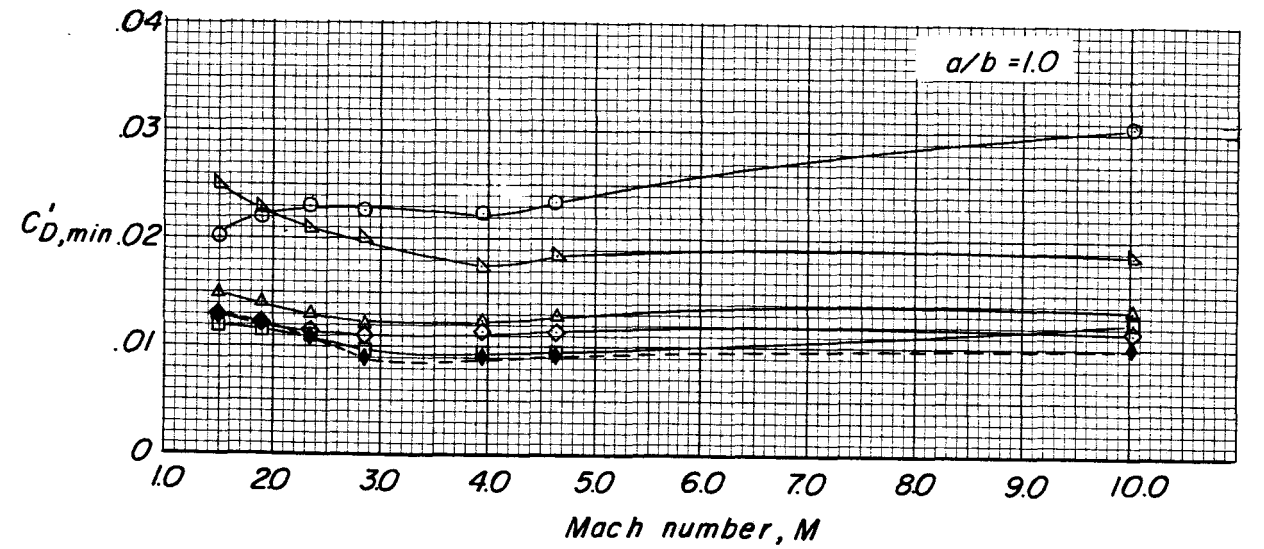

(d) Variation of $C'_{D,min}$ with Mach number.

Figure 6.- Continued.

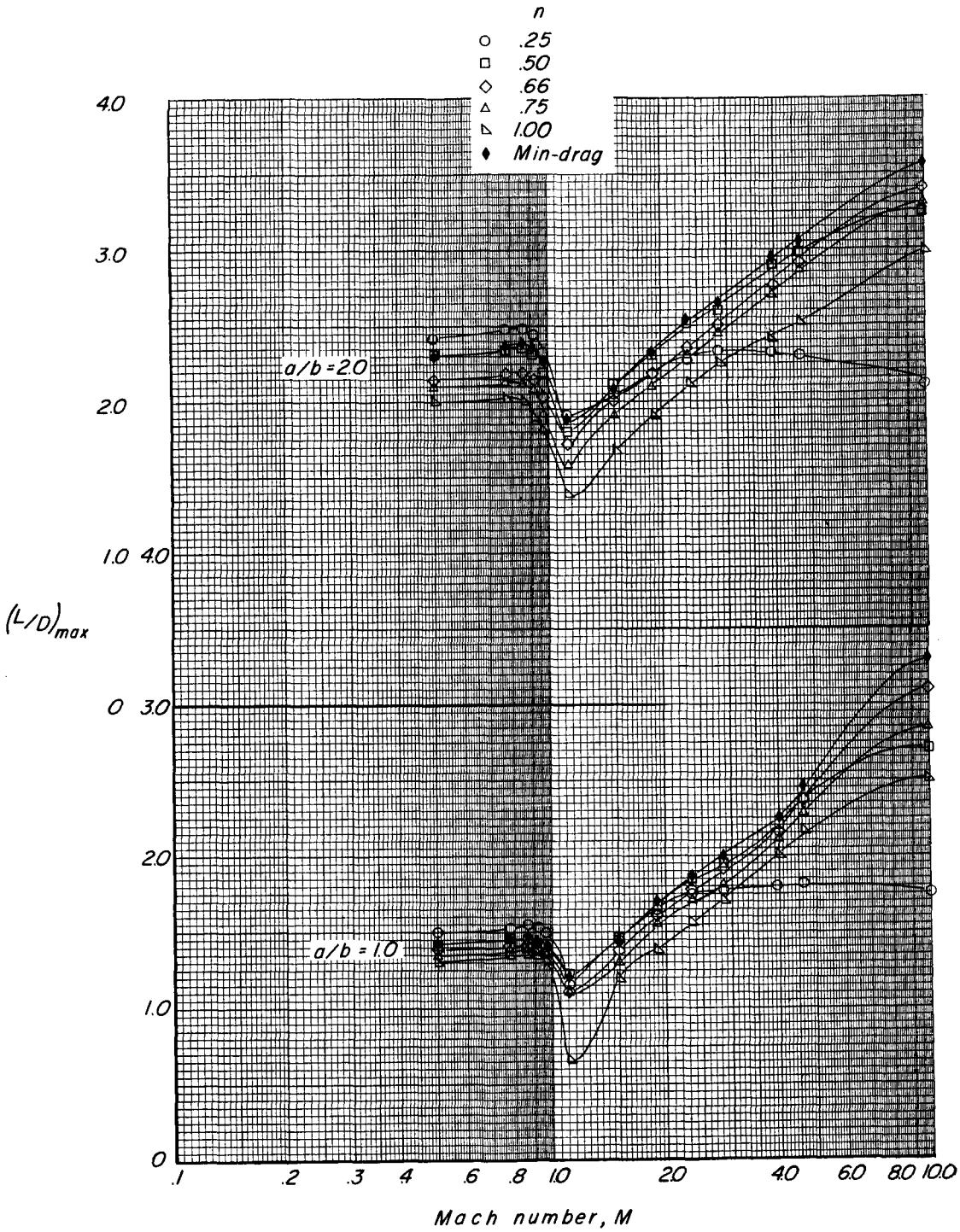

(e) Variation of $(L/D)_{max}$ with Mach number.

Figure 6.- Continued.

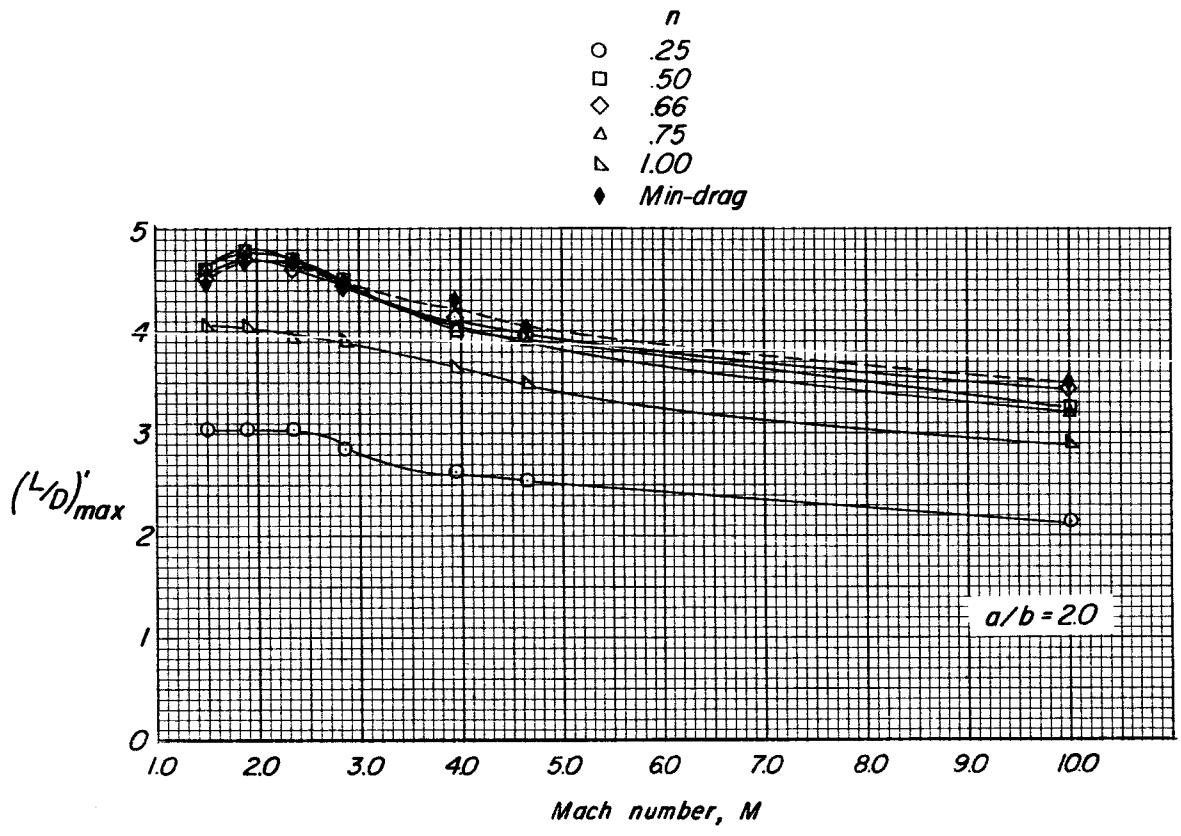

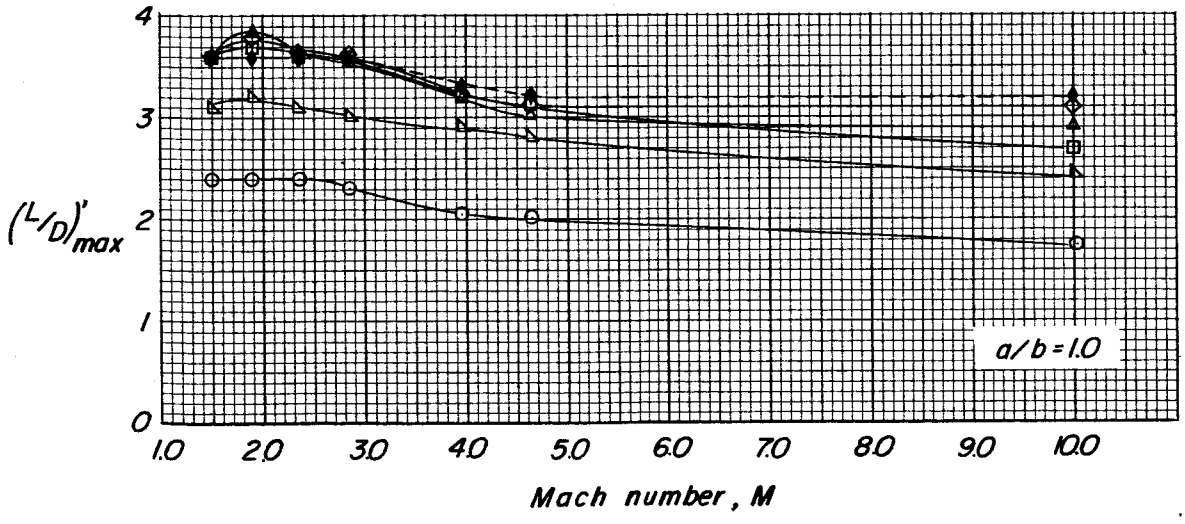

(f) Variation of $(L/D)'_{max}$ with Mach number.

Figure 6.- Concluded.

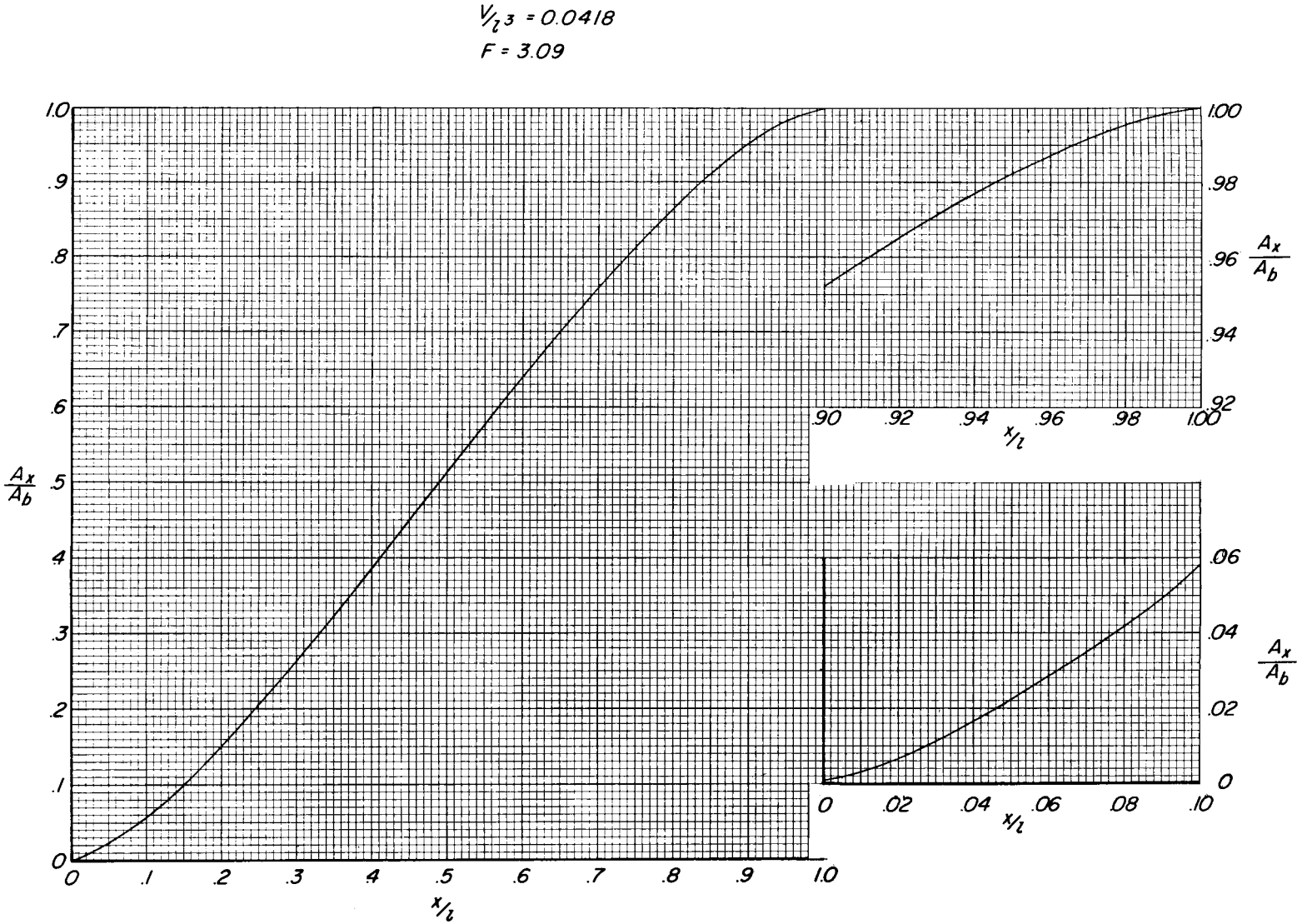

(a) Fineness-ratio-3 body.

Figure 7.- Normalized longitudinal distribution of normalized local cross-sectional area for theoretical minimum-wave-drag shape. Length and volume constraint.

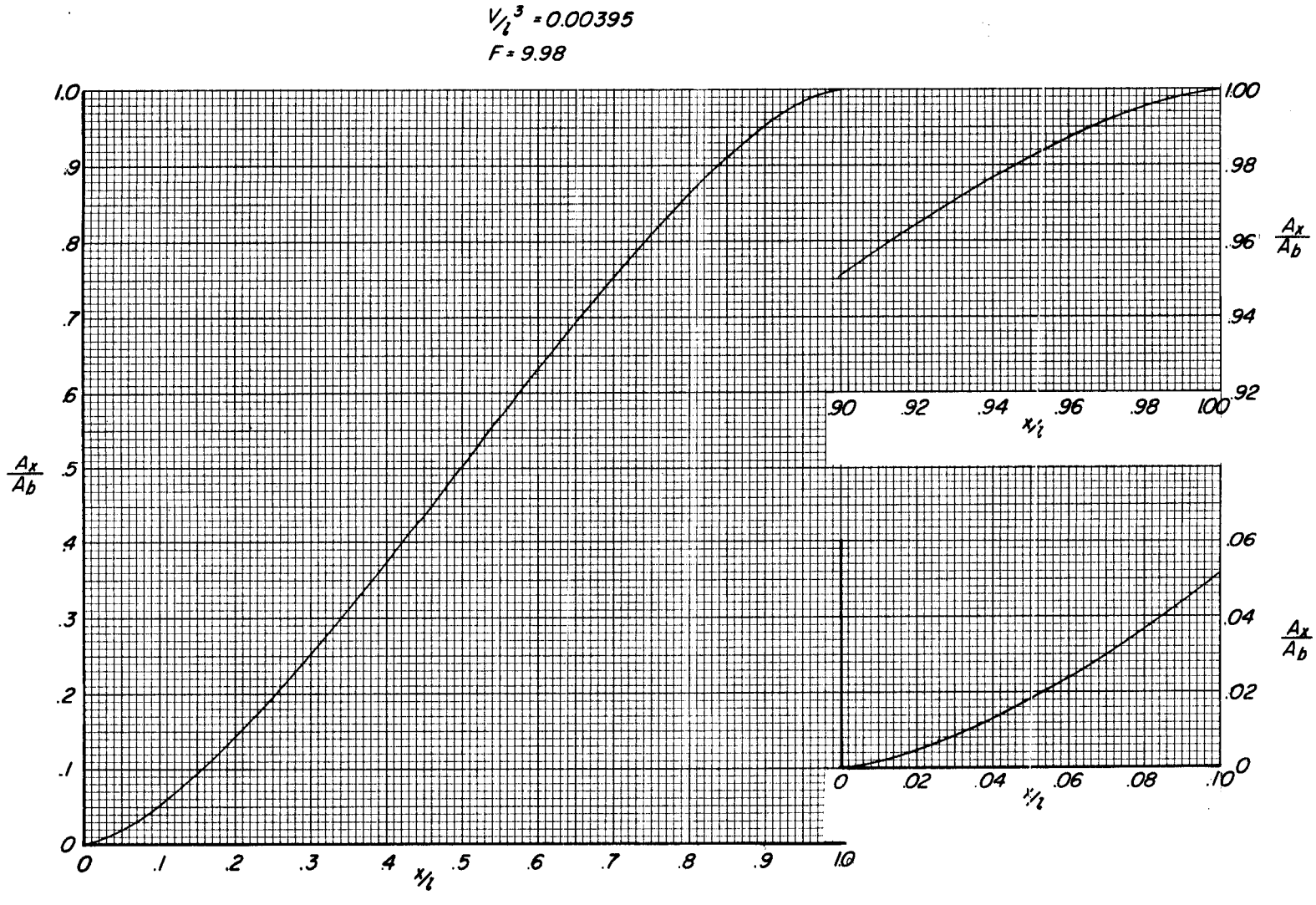

(b) Fineness-ratio-10 body.

Figure 7.- Continued.

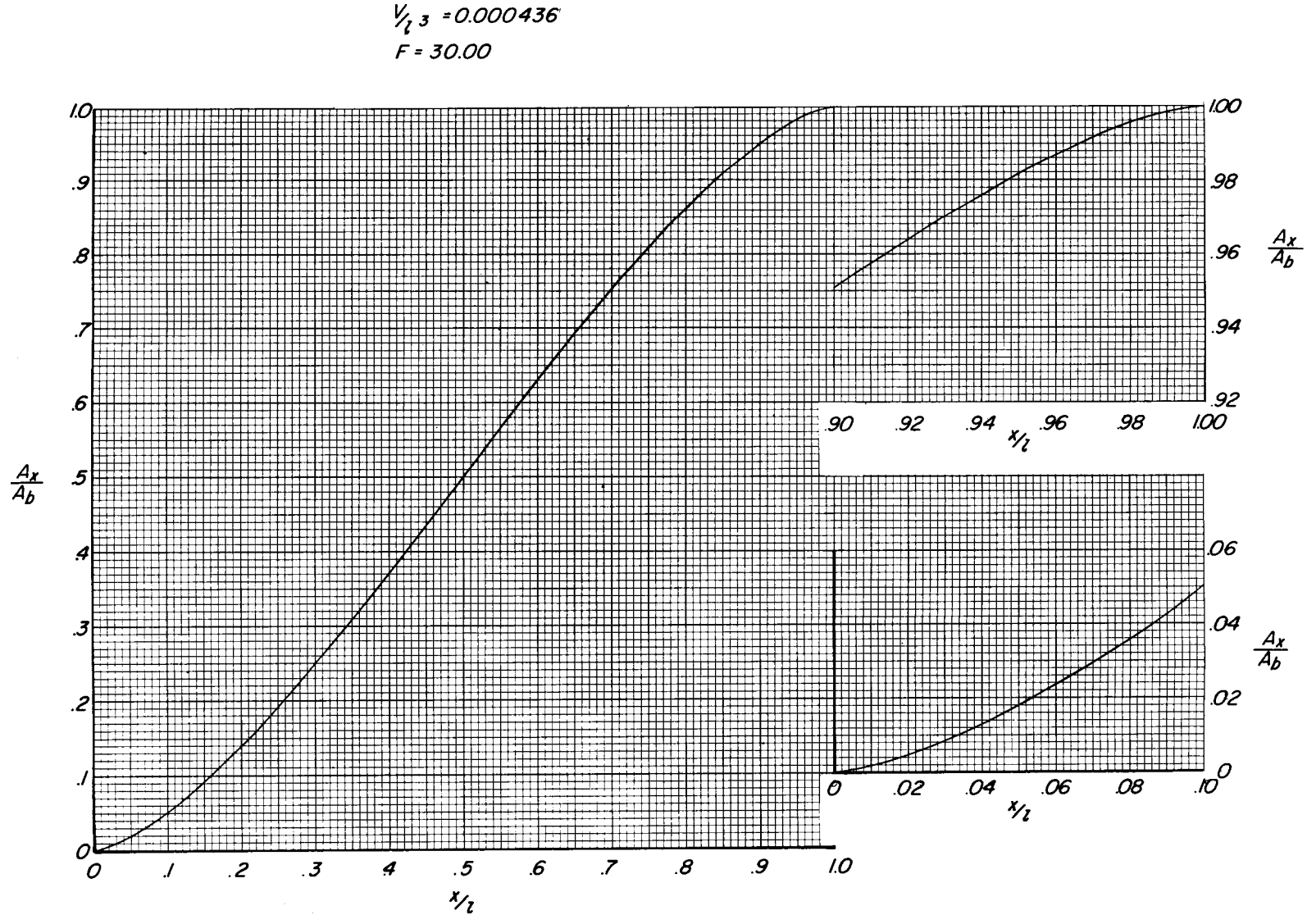

(c) Fineness-ratio-30 body.

Figure 7.- Continued.

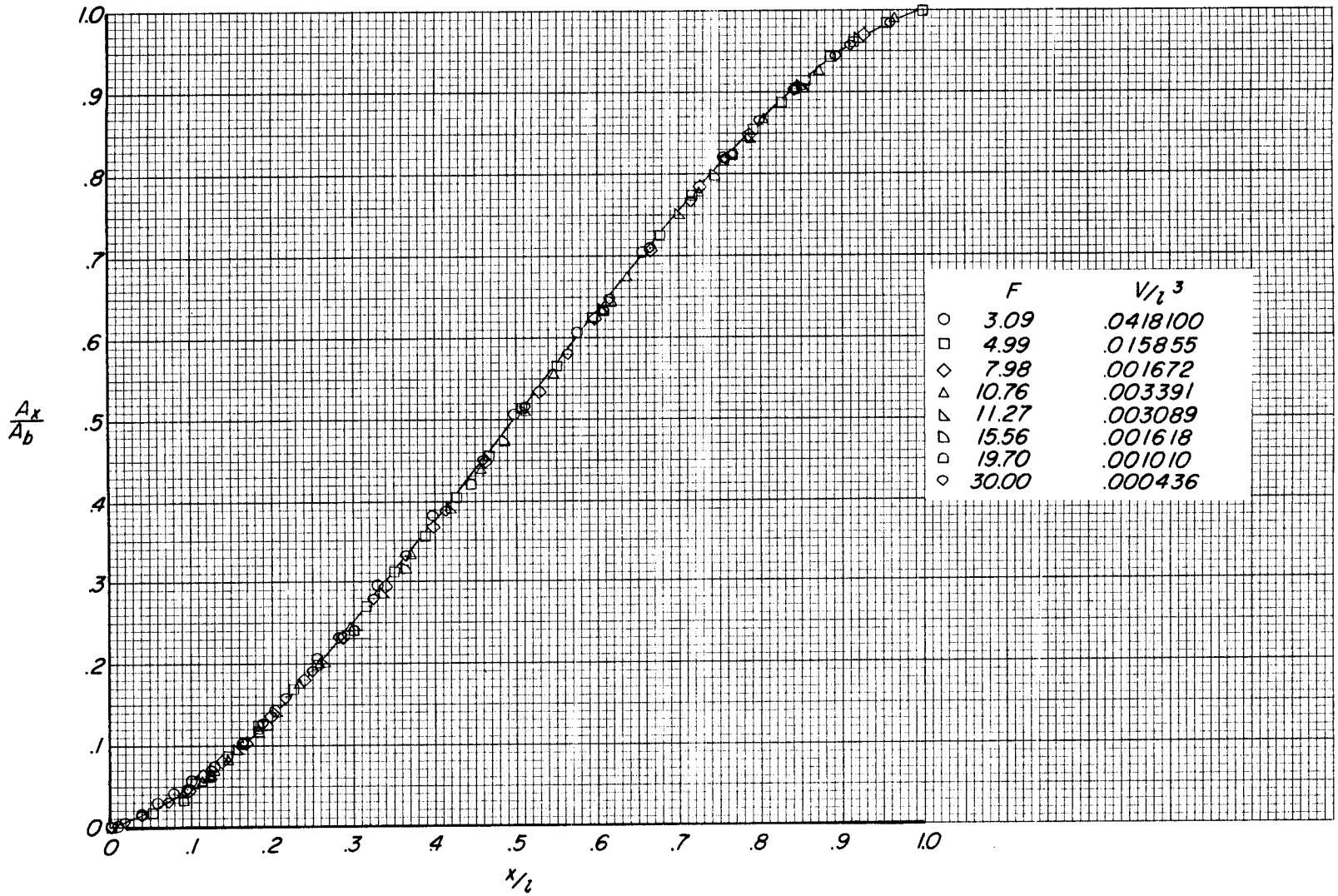

(d) Summary of results.

Figure 7.- Concluded.

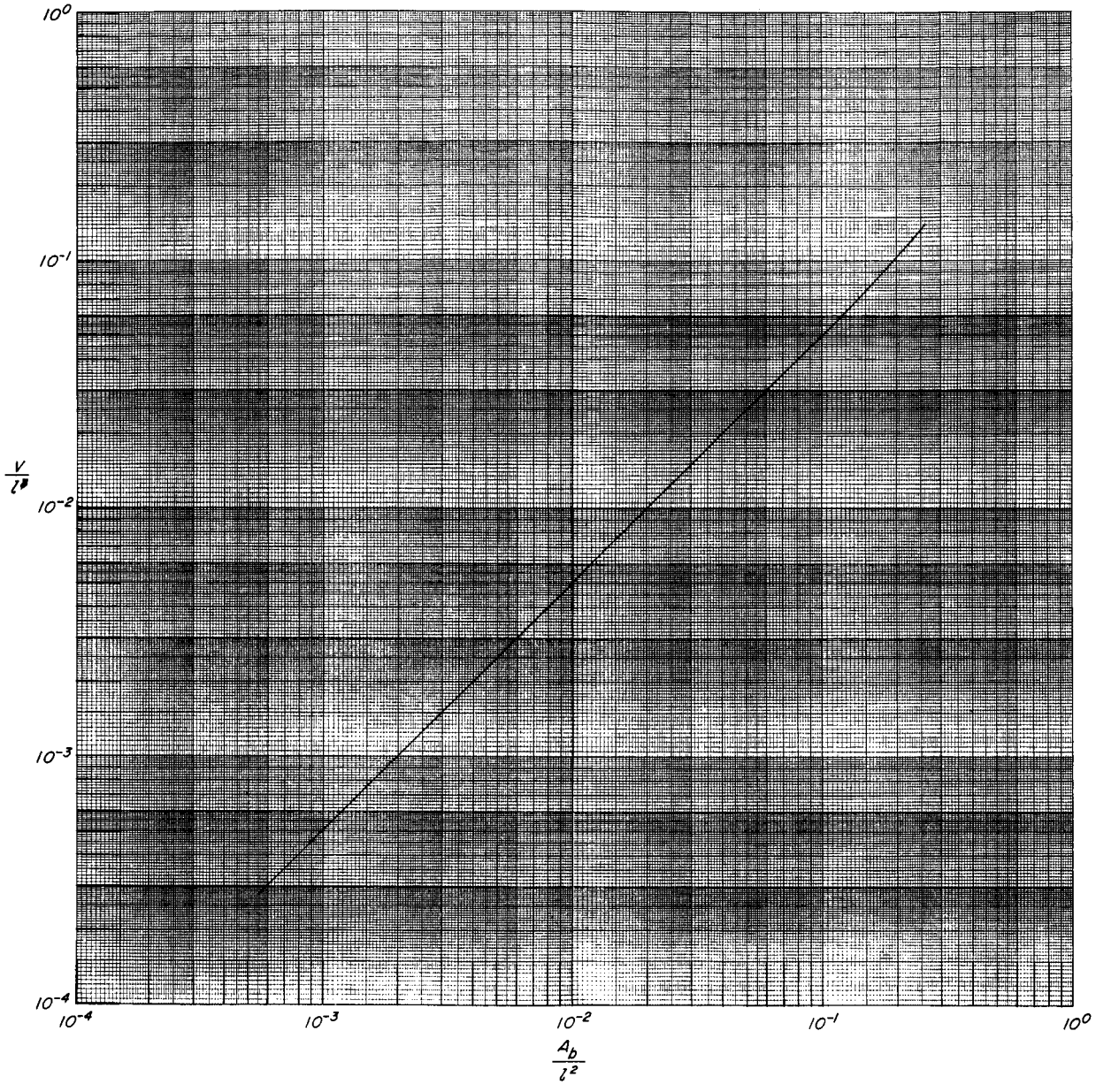

Figure 8.- The relation of the normalized base area to the volume-to-length-cubed ratio. Length and volume constraint.

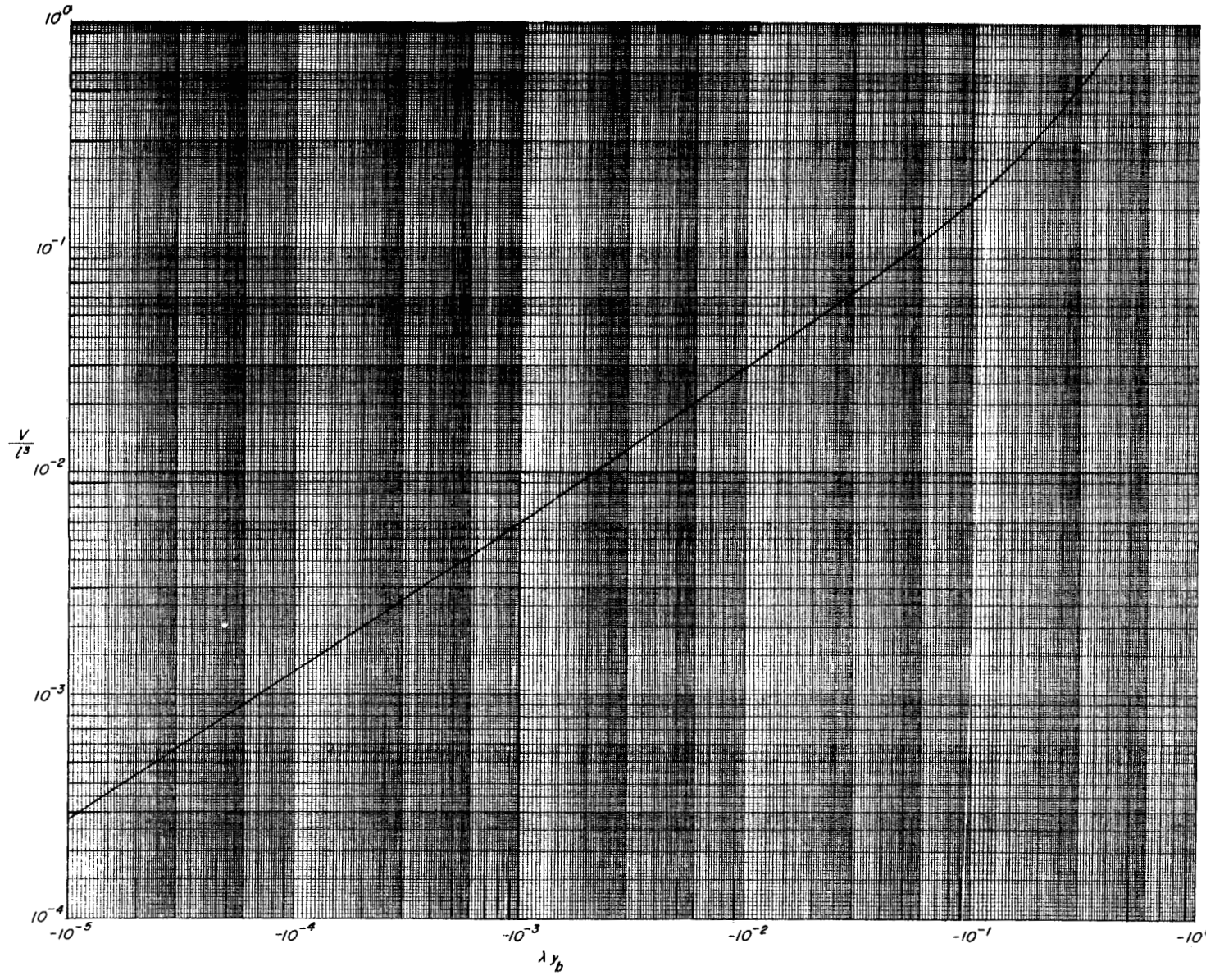

Figure 9.- The relation of the input parameter λy_b to the volume-to-length-cubed ratio. Length and volume constraint.

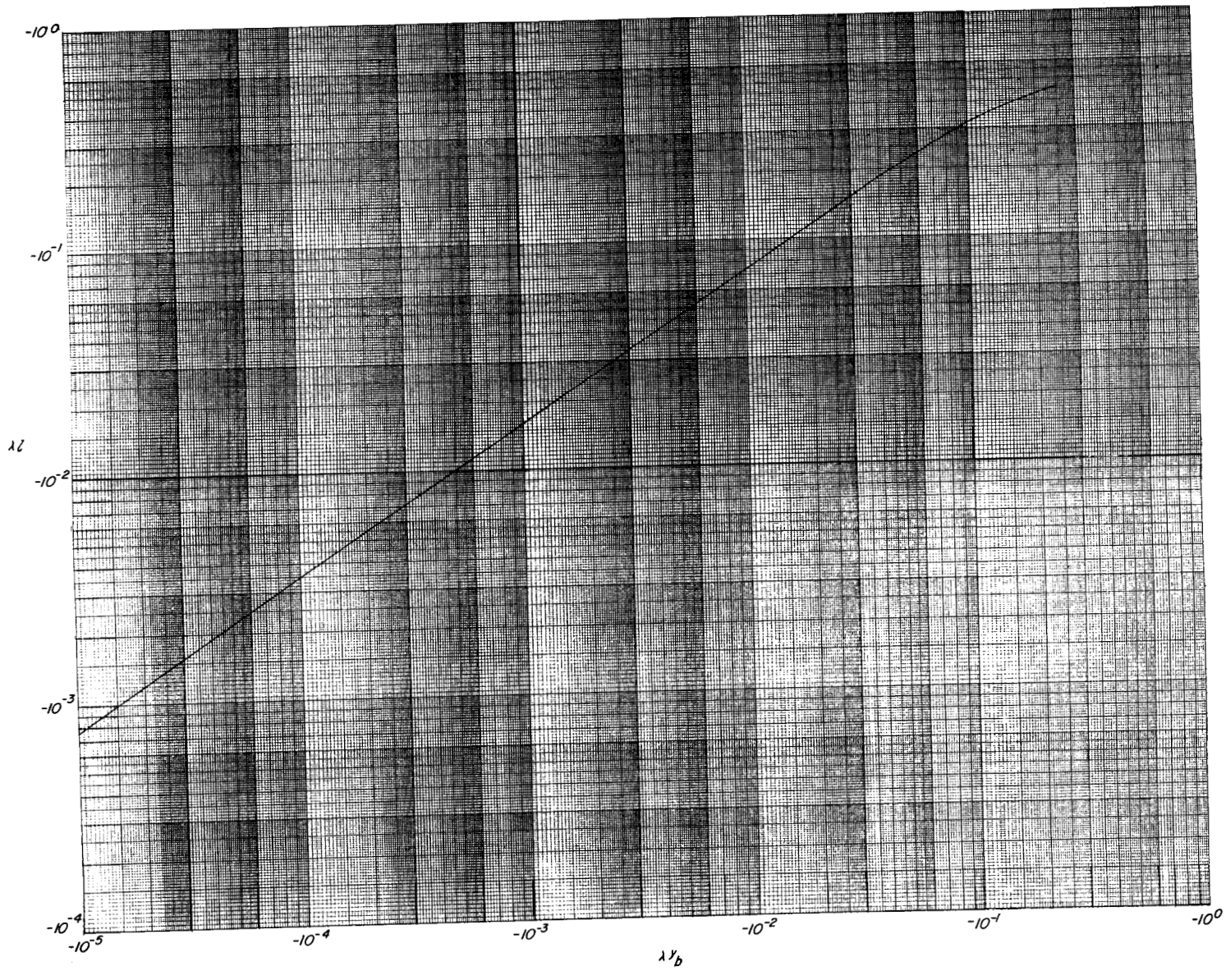

Figure 10.- The relation of the input parameter λy_b to $\lambda \ell$, used to determine λ. Length and volume constraint.

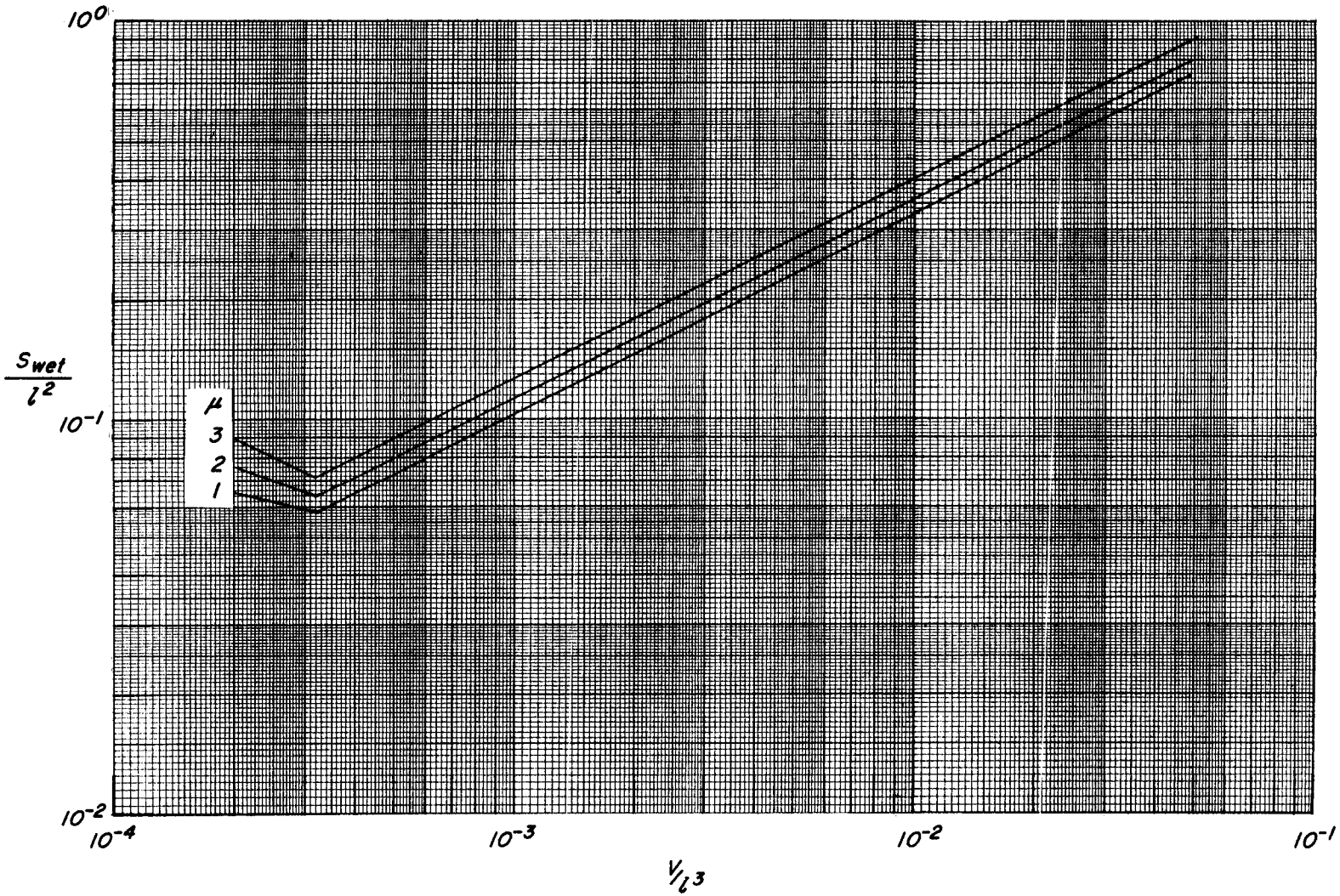

(a) Wetted area.

Figure 11.- The relation of the normalized area to the volume-to-length-cubed ratio for values of ellipticity μ of 1, 2, and 3. Length and volume constraint.

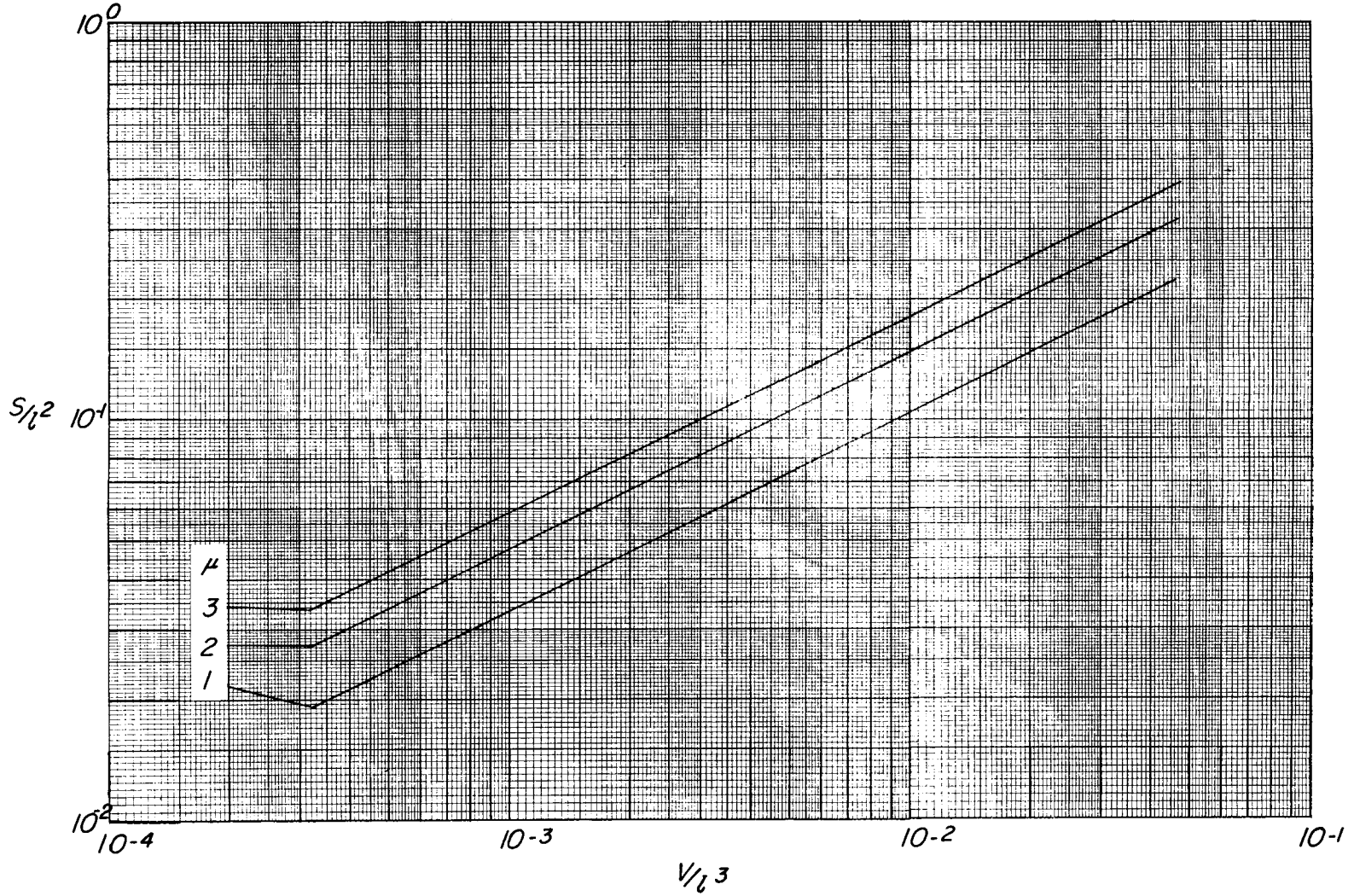

(b) Planform area.

Figure 11.- Concluded.

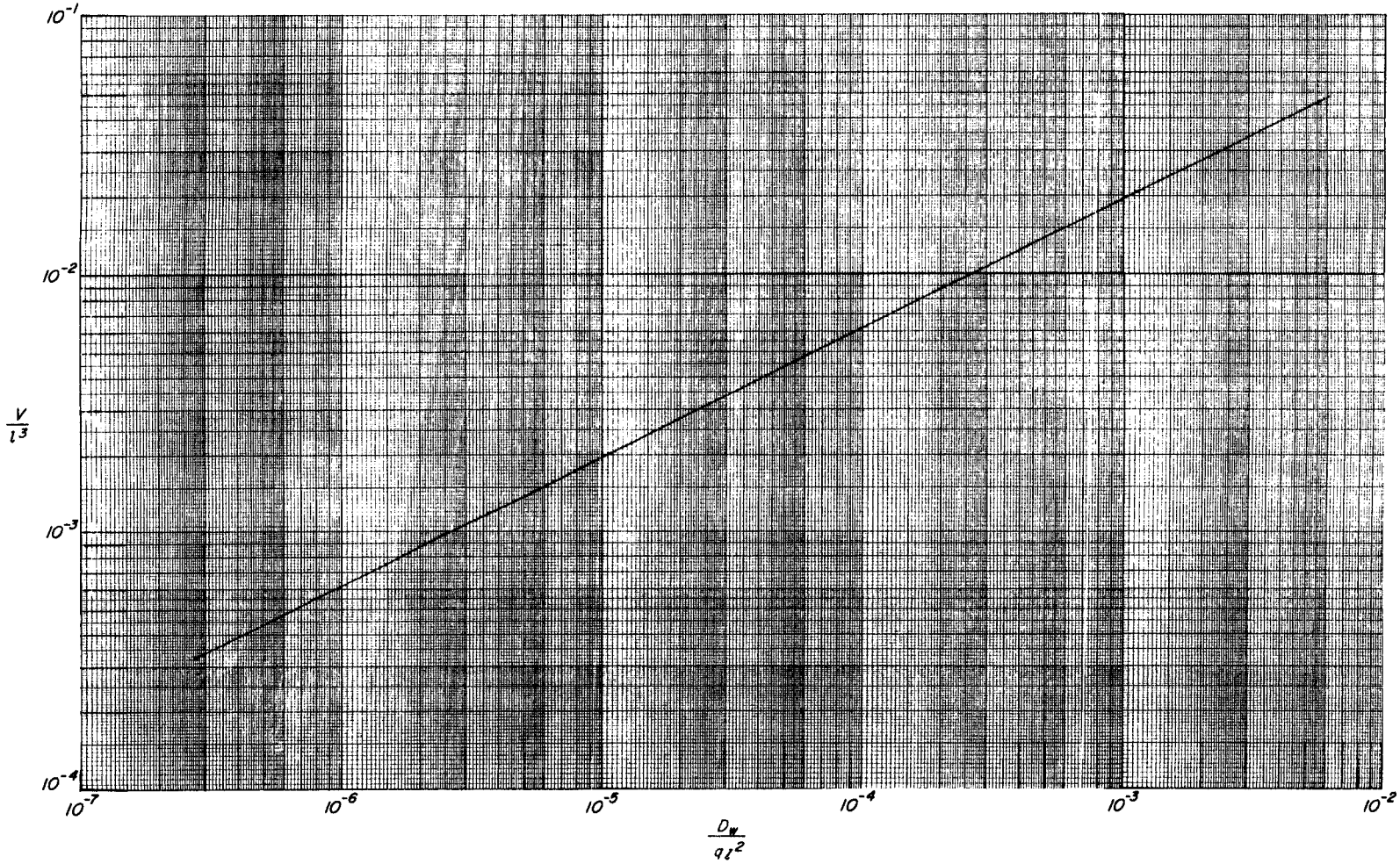

Figure 12.- The wave drag as a function of volume-to-length-cubed ratio for an ellipticity of 1. Length and volume constraint.

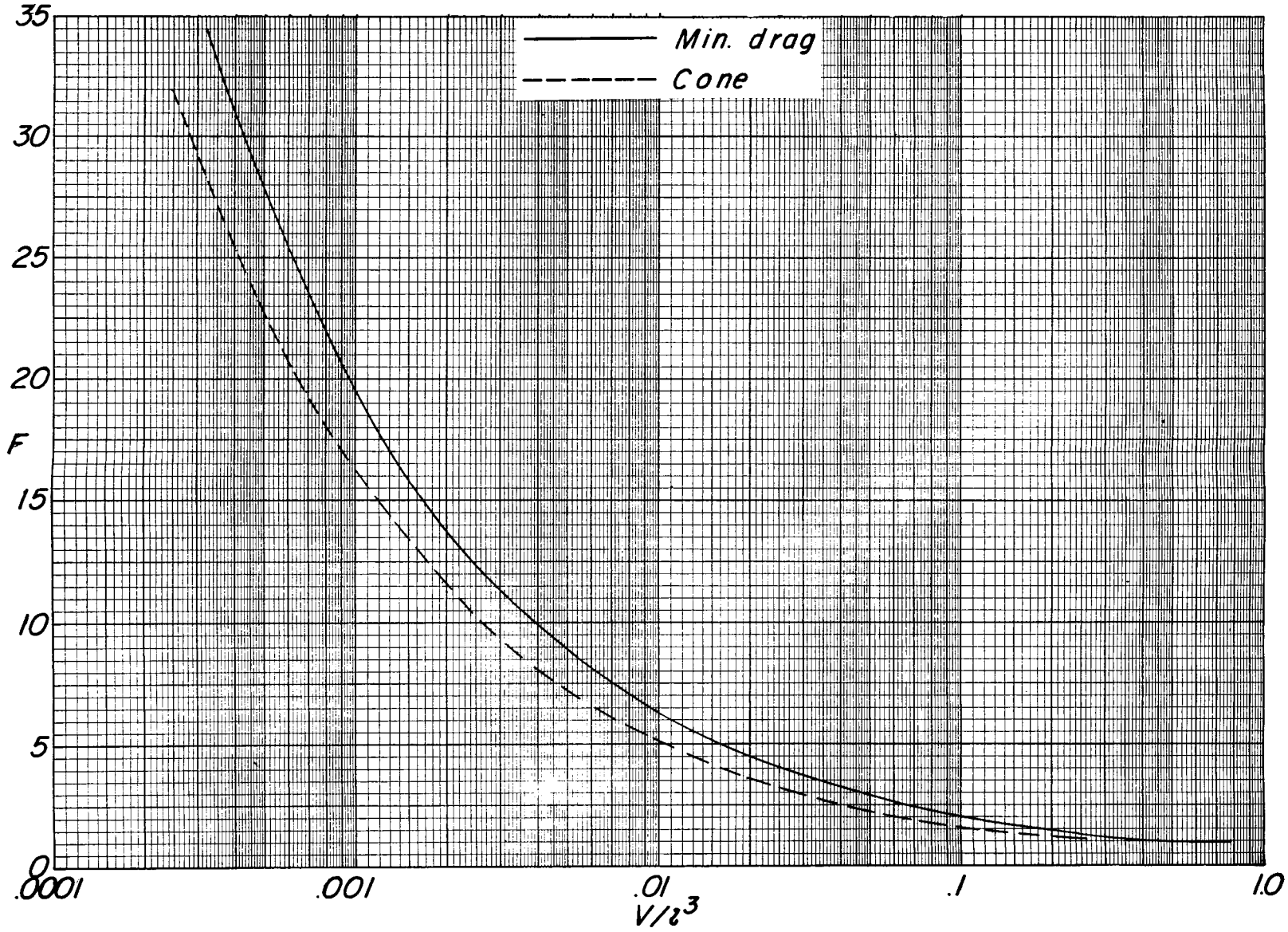

Figure 13.- Relation of fineness ratio to volume-to-length-cubed ratio for the theoretical minimum-wave-drag shape and an equivalent conical shape. Length and volume constraint.

"The aeronautical and space activities of the United States shall be conducted so as to contribute . . . to the expansion of human knowledge of phenomena in the atmosphere and space. The Administration shall provide for the widest practicable and appropriate dissemination of information concerning its activities and the results thereof."

—NATIONAL AERONAUTICS AND SPACE ACT OF 1958

NASA SCIENTIFIC AND TECHNICAL PUBLICATIONS

TECHNICAL REPORTS: Scientific and technical information considered important, complete, and a lasting contribution to existing knowledge.

TECHNICAL NOTES: Information less broad in scope but nevertheless of importance as a contribution to existing knowledge.

TECHNICAL MEMORANDUMS: Information receiving limited distribution because of preliminary data, security classification, or other reasons.

CONTRACTOR REPORTS: Technical information generated in connection with a NASA contract or grant and released under NASA auspices.

TECHNICAL TRANSLATIONS: Information published in a foreign language considered to merit NASA distribution in English.

TECHNICAL REPRINTS: Information derived from NASA activities and initially published in the form of journal articles.

SPECIAL PUBLICATIONS: Information derived from or of value to NASA activities but not necessarily reporting the results of individual NASA-programmed scientific efforts. Publications include conference proceedings, monographs, data compilations, handbooks, sourcebooks, and special bibliographies.

Details on the availability of these publications may be obtained from:

SCIENTIFIC AND TECHNICAL INFORMATION DIVISION

NATIONAL AERONAUTICS AND SPACE ADMINISTRATION

Washington, D.C. 20546